NACA TN 3764

NATIONAL ADVISORY COMMITTEE FOR AERONAUTICS

TECHNICAL NOTE 3764

NEAR NOISE FIELD OF A JET-ENGINE EXHAUST

II - CROSS CORRELATION OF SOUND PRESSURES

By Edmund E. Callaghan, Walton L. Howes, and Willard D. Coles

Lewis Flight Propulsion Laboratory
Cleveland, Ohio

Washington

September 1956

NATIONAL ADVISORY COMMITTEE FOR AERONAUTICS

TECHNICAL NOTE 3764

NEAR NOISE FIELD OF A JET-ENGINE EXHAUST

II - CROSS CORRELATION OF SOUND PRESSURES

By Edmund E. Callaghan, Walton L. Howes, and Willard D. Coles

SUMMARY

Aircraft structures located in the near noise field of a jet engine are subjected to extremely high fluctuating pressures that may cause structural fatigue. Studies of such structures have been limited by lack of knowledge of the loadings involved. In addition to the magnitude and frequency distribution of the acoustic pressures, it is necessary to know the cross correlation of the pressure over the surface area. A correlation technique has been used to determine this statistical relation in the near sound field of a large turbojet engine. Measurements with microphones were made for a range of jet velocities at locations along the jet and at a distance from the jet. Free-field correlations of the over-all sound pressure and of the sound pressure in frequency bands from 100 to 1000 cps were obtained both longitudinally and laterally. In addition, correlations were obtained with microphones mounted at the surface of a plate that was large compared with the distance over which a positive correlation existed.

The region of positive correlation was generally found to increase with distance downstream of the engine to 6.5 nozzle-exit diameters and remain nearly constant thereafter. In general, little change in the correlation curves was found as a function of jet velocity or frequency band width. The distance from unity to first zero correlation was greater for lateral than longitudinal correlations for the same conditions and locations. The correlation curves obtained in free space and on the surface of the plate were generally similar.

The results are interpreted in terms of pressure loads on surfaces.

INTRODUCTION

The extremely large acoustic radiation produced by a jet-engine exhaust has resulted in several serious problems. The far-field noise annoyance difficulties are well known (refs. 1 to 4). Another, and

perhaps more serious, problem exists in the near noise field (refs. 5 and 6). In this region, the aircraft itself is subjected to extremely high fluctuating pressures (40 lb/sq ft) that may cause structural fatigue.

Because of the importance of the structural problems created by jet noise, the NACA Lewis laboratory has undertaken an experimental investigation of the character of the sound field near the jet of a full-scale engine. The spectra and over-all sound pressures are reported in reference 7.

In order to calculate the stresses in a structure, it is necessary to know not only the acoustic pressures and spectra but also the space distribution of the pressures. In an essentially random acoustic field, such as that produced by a jet, the distribution of pressures over a surface is determined by correlation techniques. In this report, the application of correlation techniques to the determination of load distribution is discussed, and the results of correlation measurements in the near field of a full-scale turbojet engine are reported.

An electronic analog computer for determining correlation coefficients is described in the appendix by Channing C. Conger and Donald F. Berg.

Correlation measurements have been made both longitudinally and laterally to the jet (fig. 1). The majority of the measurements were made with the microphones in free space. A single set of data is given with the microphones placed in a plate of fairly large dimensions.

SYMBOLS

The following symbols are used in this report:

A	source strength
a	any fluctuating quantity
B	pressure amplitude of sound wave
c	speed of sound
d	nozzle-exit diameter
E,e	voltages
F	force
f	frequency

K,k	constants
P,p	fluctuating pressures
R	correlation coefficient
r	distance from source to receiver
s	microphone separation
T	time period over which signal was integrated
t	time
x	distance along jet centerline from nozzle exit (fig. 1)
x_1	distance along jet boundary from nozzle exit (fig. 1)
y	vertical distance from jet centerline (fig. 1)
z	horizontal distance from jet centerline (fig. 1)
α,β	phase angles
ω	angular frequency

Subscripts:

o	output
x	longitudinal
x_1	longitudinal along jet boundary
y	lateral
1,2	position or time

SOUND-PRESSURE CORRELATION

The characteristics of any noise field are usually given in terms of its time-averaged, that is, statistical, properties such as over-all sound-pressure levels and spectra. These properties are determined by measuring the root-mean-square pressures over the whole frequency range and in frequency bands. The sound pressures created by a jet are random in time, but their time-averaged products may have a spatial relation.

The usual properties of root-mean-square pressure and spectra may not be sufficient to define the load on a structure. The loading on a surface is related not only to the root-mean-square pressure at various points, but also to the degree of unison of the pressures acting over the surface. If the pressures at all points are in unison, then the root-mean-square load is simply the product of the root-mean-square pressure and the area of the surface. Usually, however, the instantaneous pressures are not in unison and the relation between the pressures is measured in terms of a statistical relation such as a correlation coefficient.

The correlation coefficient R of any two fluctuating quantities a is defined as

$$R = \frac{\overline{a_1 a_2}}{\sqrt{\overline{a_1^2}}\sqrt{\overline{a_2^2}}}$$

where the bars indicate a time average so that

$$\overline{a_1 a_2} = \lim_{T \to \infty} \frac{1}{T} \int_0^T a_1(t) a_2(t)\, dt$$

where, for practical purposes, T is a time of much longer duration than the period of the lowest frequency involved. For the case of fluctuating pressures,

$$R = \frac{\overline{p_1 p_2}}{\sqrt{\overline{p_1^2}}\sqrt{\overline{p_2^2}}}$$

where p_1 and p_2 are the instantaneous fluctuating pressure at two points.

The value of R is therefore determined by measuring the instantaneous pressures p_1 and p_2 with two microphones, obtaining their time-averaged product, and normalizing with the product of the root-mean-square values of the two pressures. In the special case where the pressures p_1 and p_2 are linearly related (act in unison), then $p_2 = kp_1$ and $R = 1$. If p_2 is completely unrelated to p_1, the product $p_1 p_2$ has equal probability of being positive or negative and, consequently, the time average of the product will be zero. Therefore, zero correlation is obtained when the relation between p_1 and p_2 is completely random. There are, however, other conditions that yield zero correlation.

The case of the sound pressures generated by a single-frequency ω simple source of strength A can be considered. If r_1 and r_2 are the respective distances of the microphones from the source, as shown in the following sketch,

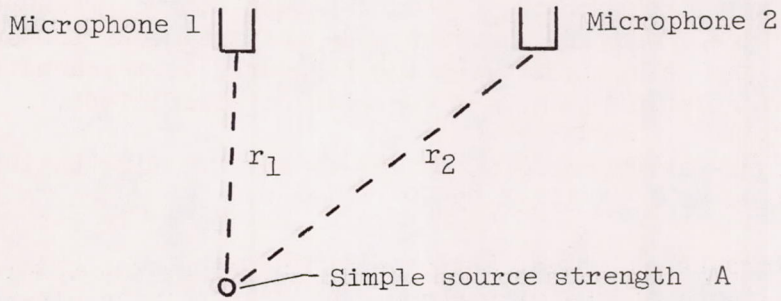

the pressures at 1 and 2 are given as

$$p_1 = \frac{A}{r_1} \cos \omega t$$

$$p_2 = \frac{A}{r_2} \cos(\omega t + \alpha)$$

The pressures at 1 and 2 are out of phase by angle α, where $\alpha = \omega(r_2 - r_1)/c$ and c is the speed of sound in the medium. The averaged product $\overline{p_1 p_2}$ is

$$\overline{p_1 p_2} = \lim_{T \to \infty} \frac{1}{T} \int_0^T \frac{A^2}{r_1 r_2} \cos \omega t \cos(\omega t + \alpha) dt = \frac{A^2}{2 r_1 r_2} \cos \alpha$$

and

$$\sqrt{\overline{p_1^2}} = \frac{A}{\sqrt{2} r_1}$$

$$\sqrt{\overline{p_2^2}} = \frac{A}{\sqrt{2} r_2}$$

Therefore, the correlation coefficient R between 1 and 2 is $\cos \alpha$. For a single frequency the correlation coefficient and the cosine of the phase angle are equivalent and, hence, can have any value from -1 to 1. There is no real necessity for limiting the previous example to a single source. Any number of sources that produce sinusoidal waves of a single frequency and random strength will induce resulting pressure fluctuations

$$p_1 = B_1 \cos \omega t$$

and

$$p_2 = B_2 \cos (\omega t + \beta)$$

at the two microphones. The coefficients B represent the resulting pressure amplitudes at the microphones, and β is a resultant phase angle. The correlation coefficient is then

$$R = \cos \beta$$

where

$$\beta = \tan^{-1} \left(\frac{A_1 \sin \alpha_1 + A_2 \sin \alpha_2 + \ldots A_n \sin \alpha_n}{A_1 \cos \alpha_1 + A_2 \cos \alpha_2 + \ldots A_n \cos \alpha_n} \right)$$

If β is 90°, then $R = 0$. Furthermore, it can be shown that, if the pressures at 1 and 2 were of two different frequencies, the correlation would always be zero.

It should be evident that, even if the sound pressures are distributed over a wide frequency range, the pressure correlation between two points results only from the relation between the identical frequency components at the two points.

If a series of correlations are determined by moving one microphone relative to another, a graph such as shown in figure 2(a) may be obtained. When the microphones are very close together, the two microphones measure the same pressure and the correlation is unity. As the microphones are separated, the correlation coefficient falls below unity. A useful equivalent to the load on a rigid surface can be determined from the correlation coefficient in the following manner: From the definition of the correlation coefficient, it follows that

$$\overline{p_1 p_2} = R \sqrt{\overline{p_1^2}} \sqrt{\overline{p_2^2}}$$

where all quantities on the right side of the equation are obtainable.

The time-averaged quantity $\overline{p_1 p_2}$ is a constant for any given microphone separation. Thus, over the total period T the constant value of $\overline{p_1 p_2}$ is equivalent to the product $P_1 P_2$ of two steady-state pressures P_1 and P_2. If a value is selected for P_1, which may be regarded as the pressure associated with the stationary microphone, then P_2 can be computed from

$$P_2 = R\sqrt{\overline{p_1^2}}\,\frac{\sqrt{\overline{p_2^2}}}{P_1}$$

where, by virtue of R, P_2 is a function of the microphone separation. Because $R = 1$ when the microphone separation is zero, $P_1 = \sqrt{\overline{p_1^2}}$ and $P_2 = \sqrt{\overline{p_2^2}} = \sqrt{\overline{p_1^2}}$. When the microphones are separated, $P_1 = \sqrt{\overline{p_1^2}}$, as before, but $P_2 = R\sqrt{\overline{p_2^2}}$ where P_2 is the most probable value of p_2 corresponding to $P_1 = \sqrt{\overline{p_1^2}}$. The last four equations permit computation of a time-average pressure distribution along a line connecting the microphones when the sound pressure at the stationary microphone is $P_1 = \sqrt{\overline{p_1^2}}$. The result amounts to replacing the random pressure distribution along the line of microphone separation by an equivalent steady-state distribution, as shown in figure 2(a).

In order to obtain a measure of the force distribution over a surface area, it is necessary to measure correlations in both the lateral and longitudinal directions (y- and x-directions, respectively, fig. 1). From such measurements, the area distribution of the pressures can be approximated in the manner shown in figure 2(b). In this figure, curves of constant P_2 have been assumed to be ellipses in planes parallel to the x,y-plane. By using such a distribution, it is possible to calculate an effective instantaneous force distribution on the plate. Before such a concept has any value, however, it must be associated with some frequency; that is, the pressure variation with time must be known.

The fluctuating pressure field near a jet is of an extremely complex character since, at any point in the field, the pressure results from a space distribution of randomly fluctuating sources. Furthermore, each source produces a fairly wide range of frequencies (ref. 7). However, the wave form of the sound at any point results from the cumulative effect of all the sources. The usual wave form in the near field of a jet has a random amplitude and a fairly peaked frequency distribution. Hence, the largest contribution to the over-all sound-pressure correlation will result from the energy centered around this peak. To a first

approximation, therefore, the loading distribution of the over-all pressures previously described might be assumed to fluctuate harmonically with a frequency corresponding to the peak frequency of the spectrum.

Surfaces in aircraft are usually resonant and would normally be expected to fail most rapidly if excited by pressure fluctuations in the band of resonant frequencies. Thus, the pressure correlations of interest in many cases are those associated with a narrow band of frequencies. The data reported herein have, therefore, been analyzed in approximately 1/2-octave bands. In order to check the 1/2-octave analyses, the correlation coefficient was also determined for a narrow band width (12 cps) with a midfrequency of 500 cps.

In order to determine the fatigue of a resonant panel, the panel should be loaded with a harmonically fluctuating load corresponding to the resonant frequency band. The amplitude of the load over the surface would be determined from the correlation curve for the band of interest and the root-mean-square pressure (in the same band). The procedure would be the same as described previously for over-all sound pressures but limited to the band width for which the plate is resonant.

The practical determination of the correlation coefficient for this investigation was obtained by the following method: The output voltage e of a microphone is linearly related to the fluctuating pressures for the range of frequencies and pressures of interest; so

$$p_1 = k_1 e_1$$

and

$$p_2 = k_2 e_2$$

and, therefore,

$$R = \frac{\overline{e_1 e_2}}{\sqrt{\overline{e_1^2}}\sqrt{\overline{e_2^2}}}$$

The correlation coefficient of sound pressures at two points in space is therefore obtained in exactly the same manner as the correlation coefficient for two fluctuating velocities in turbulence measurements (refs. 8 and 9). It is therefore possible to obtain correlation coefficients quite simply with a correlation computer of the type used in reference 9 and described in detail in the appendix of this report.

APPARATUS AND PROCEDURE

The equipment required for the determination of the space correlation of the acoustic pressures near the jet can best be described in three parts: (1) the engine and its associated equipment, (2) the equipment for obtaining and recording the acoustical data, and (3) the correlation equipment. The first two items and their use will be described in the succeeding paragraphs together with a partial description of the correlation equipment and its use. The correlation computer is described in the appendix.

Engine

The engine used for the investigation was a large axial-flow turbojet of approximately 10,000-pound-thrust rating. The exhaust nozzle was $22\frac{1}{4}$ inches in diameter. The pressure ratio across the nozzle under test-stand conditions when the engine was operated near rated power was approximately 2.2, resulting in choked flow at the nozzle and expansion to slightly supersonic flow just downstream of the nozzle. The engine was mounted in the outdoor thrust stand shown in figure 3. Engine operating conditions were chosen that would allow duplication of the engine thrust condition over the range of atmospheric conditions expected to prevail during the experiments. In addition, the time required to obtain the correlation data limited the engine operation to somewhat less than full power. All the data presented herein, unless otherwise indicated, were obtained at a thrust of approximately 9600 pounds and a jet velocity (ratio of thrust to mass flow) of 1850 feet per second. The engine was equipped with an afterburner, but it was not used for this investigation.

The engine and thrust stand were located so that no large sound-reflecting surfaces other than the ground were near the jet in any direction downstream of the engine. The engine centerline was 6 feet above ground level.

Temperature and total-pressure (velocity) surveys were made at several locations along the jet as far downstream as approximately 40 feet from the engine. From these surveys, the limits of the thermal and velocity boundaries (temperature and total pressure equal to ambient) were determined for conditions of little or no wind. Measuring stations were then set up outside the jet boundaries as shown in figure 1. These precautions were necessary to allow the acoustic data to be obtained as close to the jet as possible without subjecting the microphones to undue temperature and jet-velocity effects.

Acoustical Equipment

In order to obtain the space correlation data, it was necessary to provide a means for simultaneously recording the signals from two microphones that could be precisely located in the sound field.

Microphone positioning. - A remotely controlled and remotely indicating microphone-positioning device was used to provide the microphone movement required. One of the microphones was mounted in a fixed position to the body of the device and the other was mounted on a movable carriage. The whole assembly could be positioned at any point in the sound field outside the jet. Positioning of the fixed microphone and the traversing mechanism was accomplished by measurement from permanent markers. A photograph of the positioning device in place at one of the measuring stations behind the engine is shown in figure 4. Later in the investigation the positioner was modified to provide motion in the vertical direction.

At the beginning of each experiment, the two microphones were horizontal and adjacent with the microphone faces in the same vertical plane and at the engine centerline height. For the correlation data taken along the jet boundary (x_1-direction), this vertical plane, the a,b,c,d-plane in figure 1, was along the microphone location line. Correlation data were also obtained at three locations away from the jet boundary with the plane of the microphone faces parallel to the jet centerline (x-direction) and in the e,f,g,h-plane. For the longitudinal correlations, one microphone was moved in a horizontal direction away from the fixed microphone and toward the engine. For the lateral correlations, the microphone was moved upward from the engine centerline height.

With the microphones adjacent, the microphone centers were approximately 1 inch apart. Magnetic tape records of several minutes duration were made with the microphones adjacent for purposes of calibration of the correlation computer. The microphones were then separated in small increments and tape records of approximately 1-minute duration were taken at each position. Small increments were taken at first, and then larger increments were used when the total separation was several feet.

For the study of the longitudinal correlation over the surface of a panel, a stiff aluminum plate consisting of three segments was used as shown in figure 5. The center segment was a sliding bar approximately twice the length of the fixed top and bottom sections. The microphones were mounted behind porous, sintered stainless-steel plugs flush with the plate surface to protect the microphones. These plugs do not affect sound pressures for the range of frequencies of interest. The movable microphone was mounted near the center of the bar and the fixed microphone in the adjacent plate. The actuating and position-indicating mechanism was

similar to that previously described. The plate was mounted on vertical stands at the engine centerline height. The face of the plate was in a vertical plane along the microphone location line near the jet boundary.

Microphones. - Small condenser microphones of approximately 5/8-inch diameter were used to obtain both the free-field and plate data. Because of the differences in sound level existing at the various measuring stations, it was necessary to use several sets of microphones having appropriate sensitivities to avoid amplitude distortion of the signals. The signals from the microphones were transmitted by compensated cable systems to the recording station located in the small engine-control building (fig. 4).

Data recording. - The signals from the two microphones were recorded simultaneously on a single tape by a dual-channel magnetic-tape recorder. The signal strengths from the microphone systems were recorded at equal amplitude by controlling the recording levels separately. A cathode-ray oscilloscope was used to monitor the input signals to the recorder. From observation of the Lissajou's figures formed using both input signals simultaneously, a rough estimate of the degree to which the signals were correlated was possible during the progress of the experiments.

Data processing. - In order to determine the correlation of the data, the tapes were run through the tape-handling playback portion of the correlator described in the appendix. The dual-channel pickup heads were adjusted so that they picked up signals recorded at the same time. The correlation coefficient was then determined for each microphone separation at all the measuring stations and engine power conditions studied. These values of the correlation coefficient are over-all values for the entire frequency range of the microphone signals. Correlation of frequency-band filtered signals was also obtained. From the playback pickup system, the signals were passed through high-pass and low-pass electronic variable-frequency filters and then to the correlation computer. The frequency cutoff of the filters had a slope of 20 decibels per octave. The band width measured to the frequencies of 3-decibel attenuation for all of the frequency bands investigated is shown in the following table:

Midfrequency, cps	Frequency at 3-db attenuation, cps		Band width, cps
	Low	High	
100	80	119	39
200	161	242	81
300	244	360	116
400	326	486	160
500	405	600	195
600	485	710	225
800	650	960	310
1000	800	1200	400

In addition, one set of narrow-band filters was made that had a band-pass width of 12 cps at the 3-decibel attenuation point for a mid-frequency of 500 cps.

The limitation of the frequency bands shown (100 to 1000 cps) in the preceding table results from the frequency distribution of the sound and the limit on the maximum possible signal (voltage) level that can be impressed on the tape. The peak of the frequency spectrum occurs between 100 and 1000 cps for all the acoustical near field (ref. 7). For most positions the spectrum peak occurs near 500 cps. The available signal in each band drops off quite sharply on either side of the spectrum peak, and for most cases bands above 1000 and below 100 cps do not contain a sufficient signal for a reasonably accurate value of correlation with the computer described in the appendix. This, however, should not be particularly important since the sound pressures outside the 100- to 1000-cps region are far below the peak values (ref. 7) and probably would not have sufficient energy to affect the aircraft structure.

It would, of course, be possible to filter the microphone signal in frequency bands ahead of the recorder and, hence, obtain data over a much wider frequency range. This would result in an exceedingly large amount of engine operation time and, therefore, was not considered.

RESULTS AND DISCUSSION

The results presented herein are largely confined to the effect of various parameters, such as jet velocity and measurement position, on the correlation coefficient. All the correlation figures presented have correlation coefficient as an ordinate and a dimensionless microphone separation (ratio of microphone separation to nozzle-exit diam. s/d) as the abscissa. The data presented were obtained both longitudinally (x- or x_1-direction) and laterally (y-direction). The x_1-direction is measured along the jet boundary and is at an angle of 9.8° to the x- or axial direction (fig. 1).

Longitudinal Correlation

A typical set of correlation data is shown in figure 6. These data were obtained at a position approximately 17.3 nozzle-exit diameters downstream (measured along the jet boundary) of the engine and 12.1 nozzle-exit diameters from the jet centerline. Correlations are shown for the over-all sound pressure and for sound pressures in various frequency bands with midfrequencies from 100 to 1000 cps. The width of each band and its midfrequency is tabulated in the APPARATUS AND PROCEDURE section.

The correlation curves of figure 6 show interesting characteristics. There is a definite order to the results. The higher midfrequencies show a decreased region of positive initial correlation. The microphone separation for which the correlation coefficient is initially zero occurs at decreasing s/d values, and the curves sharply steepen with increase in frequency. The maximum negative correlation and the second zero-correlation points follow this same trend. Decreasing frequency results in a movement of both the maximum negative and the second zero correlation toward larger values of s/d. The maximum negative correlations show a definite tendency to increase (negatively) to a midfrequency of 400 cps and to decrease thereafter.

For the data shown in figure 6, the peak of the frequency spectrum occurs between 300 and 400 cps. The over-all correlation curve also falls between the 300- and 400-cps midfrequency correlation curves. All the correlation data exhibited this characteristic; that is, the over-all correlation curve fell near the correlation curves corresponding to the peak of the spectrum. The approximation of the over-all curve by a curve of single frequency as described previously in the section SOUND PRESSURE CORRELATION would appear to be useful for structural loading purposes.

Effect of jet velocity. - The over-all sound-pressure correlation for a range of jet velocities from 630 to 1780 feet per second is shown in figure 7. These data were obtained along the jet boundary 2.16 nozzle-exit diameters downstream of the nozzle exit. In general, the shapes of the curves are nearly the same, and the effect of jet velocity appears to be quite small.

The small effect of velocity might well be inferred from the results of reference 9, which show very little effect of exit velocity on the scale and intensity of turbulence. Since the relation of the sound-pressure spectrum near the jet is quite similar to the turbulent velocity spectrum in the jet (ref. 7), it would be expected that the near-field sound would reflect the same trends as the turbulence results.

The effect of velocity on the correlation coefficient for several frequency band widths is shown in figure 8. As might be expected from the previously discussed results on the over-all sound-pressure correlation, the effect of velocity on the correlation for the various band widths is quite small.

Effect of position. - The correlation of the over-all sound pressures at various positions along the jet boundary is shown in figure 9. Near the nozzle exit, 2.16 nozzle-exit diameters downstream along the boundary, the region of positive correlation extends to an s/d value of 0.385. Farther downstream the region of positive correlation increases, but at 6.5, 10.8, and 17.3 nozzle-exit diameters the region of positive correlation is nearly the same and appears to give a first zero crossing at about s/d of 0.93. The correlation of these same data for the various

frequency bands is shown in figure 10. In general, the correlations of figure 10 follow the general trend of decreasing region of positive correlation with increasing frequency, as discussed previously (fig. 6). This is shown quite clearly in figure 11, where the initial zero-crossing point (fig. 10) is plotted as a function of frequency. The straight line relation of the data indicates that the distance for initial zero crossing is related to the frequency by an equation of the form

$$s/d = \frac{k}{(\text{frequency})^n}$$

The value of n appears to increase nonuniformly from about 0.5 near the nozzle to about 1.2 far downstream.

The results shown in figure 10, however, do not show exactly the same order as the correlations of over-all sound pressures in figure 9. This should be expected since the spectrum distribution of the sound changes in moving downstream from the nozzle exit. The peak of the sound-pressure spectrum curve occurs at decreasing frequency with increasing downstream distance (ref. 7). If space and time are related by an eddy convective velocity or the speed of sound, the correlation of the over-all sound pressures can be achieved from the Fourier transform of the sound-pressure spectrum. It should be expected, therefore, that the shift in the spectrum would show up in the band-pass correlations.

In figure 12 is shown a comparison of over-all sound-pressure correlations measured on the jet boundary and 12.1 nozzle-exit diameters from the jet centerline for two downstream distances. At a downstream distance of 6.5 nozzle-exit diameters, the shape of the correlation curves are vastly different. On the boundary, the first zero-correlation position occurs at an s/d value near 0.85, whereas 12.1 nozzle-exit diameters from the jet the correlation coefficient appears to approach zero asymptotically. At 17.3 nozzle-exit diameters downstream of the nozzle exit, the curves are somewhat similar, although the microphone separation at the first zero crossing is slightly larger near the jet. The data of figure 12 in the various bands are also shown in figures 6 and 10 except for the position 6.5 nozzle-exit diameters downstream of the nozzle exit and 12.1 nozzle-exit diameters from the centerline. These correlations are presented in figure 13.

Effect of band width. - The correlation of sound pressures would ideally be made for a band width corresponding to the band width to which the surface is responsive. This would not necessarily be worthwhile, as illustrated in figure 14. In this figure, data at several locations in the field are presented for two band widths, 195 and 12 cps, both having essentially the same midfrequency (500 cps). It is evident that the initial region of positive correlation is practically independent of the

width of the band pass for a band pass less than 1 octave. There is a tendency when reducing the band width for an increase in the maximum negative value of the correlation coefficient but little effect on the positions where the values of first zero crossing occur. The small effect of decreasing the band width from 195 to 12 cps indicates that further decreases in the band-pass width would show only an increase in the absolute magnitude of the second maximum positive and negative values but little change in the zero-crossing positions. This result agrees with a similar treatment of turbulence data (ref. 9). It should be obvious that increasing the band width by an appreciable amount is bound to shift the curves toward the over-all sound-pressure correlation.

Comparison of free field and plate. - The results presented thus far have been concerned with the correlation in free field. A point of considerable interest is the relation between a free-field correlation and a correlation on a surface. It might be expected that the introduction of a surface into a sound field would cause some change in the correlation.

As a preliminary estimate of this effect, a single set of data was obtained of the correlation on a flat plate. The dimensions of the plate and the microphone locations are shown in figure 5. The data were obtained with the fixed microphone located approximately 2.7 nozzle-exit diameters downstream of the nozzle exit, the long dimension of the plate along the jet boundary, and with the plate surface tangent to the jet. From figure 9 it can be seen that the free-field over-all sound-pressure correlation is much smaller than the physical dimensions of the plate; that is, the correlation has become nearly zero in the first 0.9 nozzle-exit diameters compared with the plate length of 1.98 nozzle-exit diameters.

The over-all sound-pressure correlation coefficient for both the plate and free field at approximately the same spatial location is shown in figure 15. Also shown in the figure are the results for several frequency bands. From these data it can be seen that the surface correlation and the free-field correlation for each frequency are not too different. The correlation curves for the plate have slightly different shapes and greater negative values than the free-field results. This might well be caused by the slightly different locations of the plate and free-space measurements. The plate location (fixed microphone) was approximately 1 foot downstream of the free-field measurements. It would appear, therefore, that correlation is relatively unaffected by the presence of the body in the field, at least for the case where the body is larger than the area over which the pressures are correlated to a large degree.

It is interesting to note that the actual sound-pressure levels on the plate (when placed along the jet boundary) are much higher than those measured in the free field (ref. 7).

Lateral Correlation

In general, it would be expected that a sound-pressure correlation would involve a spatial volume. That is, a constant value of the correlation coefficient would have a shape in space in the same sense that a turbulence correlation has in a jet (ref. 9). For structural considerations, it is necessary to know the correlation in the plane of the surface under consideration. Measurements have therefore been made along a vertical line (y-direction, fig. 1) at several positions corresponding to measurement points of longitudinal correlation. No measurements were made in the direction normal to the plane of the longitudinal and lateral correlations.

Effect of position. - Correlations of the over-all sound pressures at three positions are shown in figure 16. In each case the fixed microphone was held in the horizontal plane of the jet centerline (fig. 1) and the movable microphone was moved vertically upward.

It is apparent from the figure that the pressures are correlated over a considerable distance. In fact, only the data at 2.16 nozzle-exit diameters downstream along the jet boundary show a zero correlation within the actuator limits. If the data of figure 16 are compared with the longitudinal correlations for the two comparable space positions (fig. 9), it is apparent that the lateral distance to the first zero crossing is larger than the longitudinal.

A single set of measurements moving the microphone vertically downward were made at 2.16 nozzle-exit diameters downstream along the jet boundary. These data were nearly identical to the results obtained when moving the microphone upward.

Correlation in frequency bands. - The correlation in frequency bands at 17.3 nozzle-exit diameters downstream is shown in figure 17. These data show exactly the same trends as the longitudinal correlations in frequency bands (fig. 6).

Effect of band width. - The effect of band-pass width on the correlation for two frequency bands at two downstream distances is shown in figure 18. It is apparent that the effect of band-pass width is quite small in the initial positive region. The maximum negative value is greater for the smaller pass band, which agrees with the effect on longitudinal correlations presented in figure 14.

SUMMARY OF RESULTS

As part of the study of the near noise field of a jet exhaust, the space correlations of the sound pressures have been measured and the following results obtained:

1. The size of the region of positive longitudinal correlation of the over-all pressures along the jet boundary (the distance to the first zero crossing of the correlation curves) varied from 0.385 to 0.93 nozzle-exit diameters.

2. Longitudinal correlation curves obtained over a range of jet velocities from 630 to 1730 feet per second showed, in general, little change in the over-all and frequency band-width correlations as a function of jet velocity.

3. For longitudinal correlations along the jet boundary the first zero-crossing distance was found to increase with distance from the engine up to about 6.5 nozzle-exit diameters. However, at distances of 6.5, 10.8, and 17.3 nozzle-exit diameters downstream from the engine, there was little difference in the first zero crossing distance.

4. Longitudinal correlations measured 12.1 nozzle-exit diameters from the jet centerline at a distance downstream of 6.5 nozzle-exit diameters from the nozzle exit approached zero asymptotically. Farther downstream from the exit (17.3 nozzle-exit diam), the correlation curves measured 12.1 nozzle-exit diameters from the jet centerline were more nearly like those at the jet boundary.

5. A comparison of the correlation curves obtained at a midfrequency of 500 cps for band widths of 12 and 195 cps showed small effect of band width. The narrow band resulted in increases in the second maximums and minimums, but no significant change occurred in the zero-correlation distance.

6. Correlation curves obtained in free field and on the surface of a plate showed only minor dissimilarity.

7. The distance over which the correlation coefficients were positive was greater for lateral than for longitudinal correlations.

Lewis Flight Propulsion Laboratory
National Advisory Committee for Aeronautics
Cleveland, Ohio, May 25, 1956

APPENDIX - CORRELATION COMPUTER

By Channing C. Conger and Donald F. Berg

The correlation computer is a device that is designed to solve by analog methods an equation of the form

$$E_o = \frac{K}{T} \int_0^T e_a(t) e_b(t) dt \tag{1}$$

where T is real time, E_o is the output voltage from the computer, and e_a and e_b are the input voltages. The correlation of two voltages may be written as

$$R = \frac{1}{\sqrt{\overline{e_a^2}\,\overline{e_b^2}}} \frac{1}{T} \int_0^T e_a e_b \, dt \tag{2}$$

where the bar indicates the true time average. Therefore, if K is made equal to $1/\sqrt{\overline{e_a^2}\,\overline{e_b^2}}$, then $E_o = R$. If $e_b(t) = e_a(t + \Delta t)$, where Δt is a time delay, then R is termed the autocorrelation coefficient of e_a.

The operation of the computer will be described with reference to figure 19. The two signals whose correlation is to be measured are recorded on a dual-channel tape recorder on 1/4-inch magnetic tape. The signals are recorded in periods of from 1 to 30 minutes followed by 10-second intervals during which nothing is recorded on the tape. All tape-recording equipment is commercially available and of instrument quality.

The magnetic tape is played back on a tape handler similar to the one used in recording but with a special playback head arrangement. The playback heads are mounted so that one of the two heads may be translated along the tape with respect to the other. The amount of translation is measured by a micrometer head used to drive the movable playback head. The maximum head motion is 3/4 inch, and this motion may be measured to an accuracy of 1×10^{-4} inch by means of a vernier on the micrometer head. The tape speed used on playback is 15 inches per second. Therefore, the adjustment allows an adjustable delay of from 0 to 50 milliseconds to be introduced between the signals from the two playback heads. This adjustable delay is used in the determination of autocorrelation functions as described previously. For cross correlations (as from two microphones), the delay is adjusted to zero.

The compensation amplifiers receive the two signals from the playback heads. The gain characteristics of these amplifiers have been adjusted by means of passive filters to compensate for the frequency characteristics of the recording system. They also serve to correct for the frequency response of the playback heads and to amplify the signals to a level suitable for use by the remainder of the circuitry. From the compensating amplifiers, the signals go to the variable-gain amplifiers, as shown in the block diagram. The adjustable-gain feature of these amplifiers is used to set the scaling coefficient K of equation (1).

The switching circuit (indicated in fig. 19) is used to switch the output voltages of the variable-gain amplifiers to a monitering oscilloscope, a vacuum-tube voltmeter, or the electronic multiplier. The switching circuit aids in setting up the computer and in checking its operations during use.

From the switching circuit, the two signals are applied to the electronic multiplier. The multiplier produces an output voltage proportional to the instantaneous product of the input voltages. The product voltage is applied to resistance-capacitance averaging circuit of conventional design. The average amplitude of the product voltage is then read from the vacuum-tube voltmeter.

When used for autocorrelation measurements, the computer is usually adjusted so that the correlation may be read directly from the voltmeter. The adjustment consists of the following: The heads are adjusted until zero time lag is produced; therefore, the correlation is unity. Then, the gain of the variable-gain amplifiers is adjusted until the output of the multiplier indicates 1 volt full scale on the voltmeter. With this initial setting, the autocorrelation coefficient may be read directly from the voltmeter dial as a function of the time delay obtained by adjusting the movable head.

Two blocks of figure 19 remain to be described, the calibration circuit and the tape-reversal control. The calibration circuit provides appropriate alternating-current and direct-current voltages that may be switched into the electronic multiplier. These voltages are used for calibration and adjustment of the multiplier prior to use.

The tape-reversal control is used to operate automatically the tape handler. The control uses the 10-second blank intervals at the end and beginning of a section of recorded data on the tape to stop automatically, rewind, and restart the tape handler. Use of the controller, therefore, allows a section of the tape to be played back repeatedly without attention from the operator and produces the effect of a loop of tape without the necessity of cutting and splicing the tape.

Complete circuits of the correlation computer showing the construction of electronic portions of the equipment (and the amplifier response curves) are presented in figures 20 to 27 and table I.

REFERENCES

1. Bolt, Richard H.: Aircraft Noise and Its Relation to Man. Paper presented at Inst. Aero. Sci. meeting, Cleveland (Ohio), Mar. 12, 1954.

2. Bolt, Richard H.: Aircraft Noise Problem. Jour. Acoustical Soc. Am., vol. 25, no. 3, May 1953, pp. 363-366.

3. Stevens, K. N.: A Survey of Background and Aircraft Noise in Communities Near Airports. NACA TN 3379, 1954.

4. Hubbard, Harvey H.: A Survey of the Aircraft Noise Problem with Special Reference to Its Physical Aspects. NACA TN 2701, 1952.

5. Miles, John W.: On Structural Fatigue Under Random Loading. Jour. Aero. Sci., vol. 21, no. 11, Nov. 1954, pp. 753-762.

6. Powell, Alan: The Problem of Structural Failure Due to Jet Noise. Oscillation Sub-Committee, British A.R.C. 17514, Mar. 29, 1955.

7. Howes, Walton L., and Mull, Harold R.: Near Noise Field of a Jet-Engine Exhaust. I - Sound Pressures. NACA TN 3763, 1956.

8. Laurence, James C., and Landes, L. Gene: Auxiliary Equipment and Techniques for Adapting the Constant-Temperature Hot-Wire Anemometer to Specific Problems in Air-Flow Measurements. NACA TN 2843, 1952.

9. Laurence, James C.: Intensity, Scale, and Spectra of Turbulence in Mixing Region of Free Subsonic Jet. NACA TN 3561, 1955.

TABLE I. - SWITCH POSITION FOR SWITCHING CIRCUIT

Switch position	Meter signal proportional to
1	X,Y,Z
2	Y,Z^2
3	X,Z^2
4	X,Y^2
5	Z,Y^2
6	Z,X^2
7	Y,X^2
8	Y,Z
9	X,Y
10	X,Z
11	Z^2
12	Y^2
13	X^2

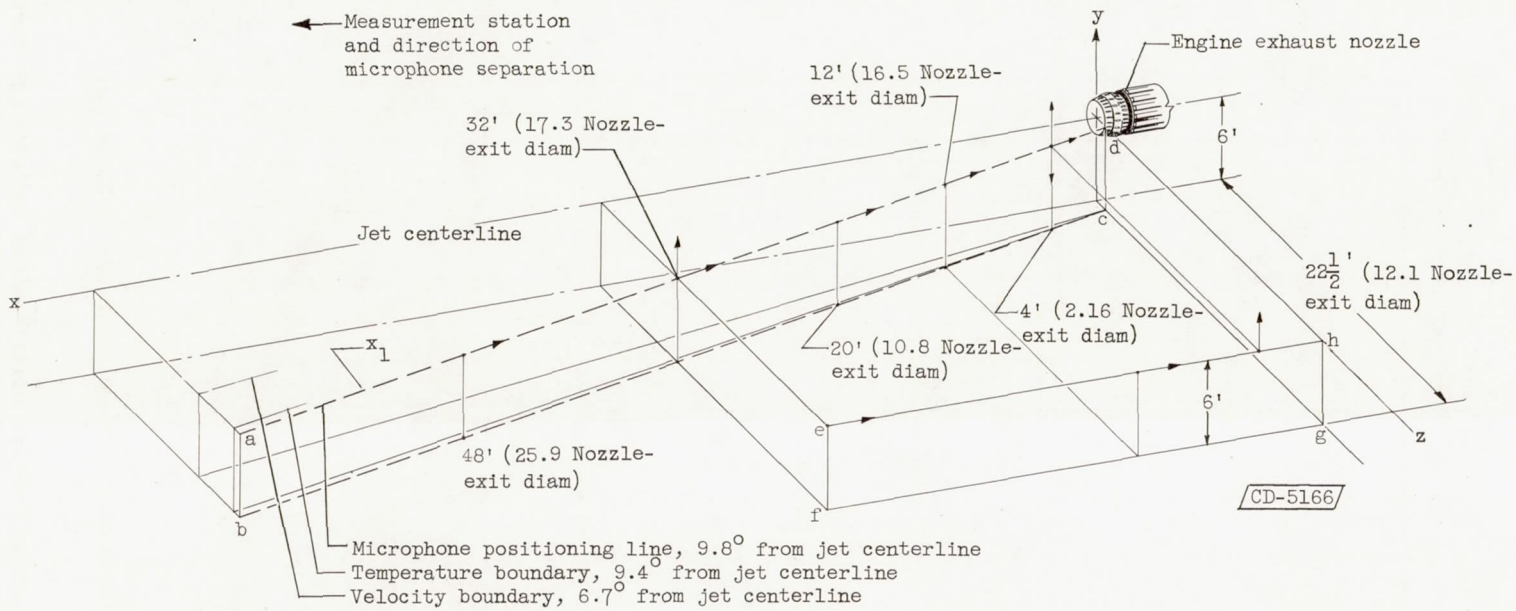

Figure 1. - Location of jet boundaries and measurement stations.

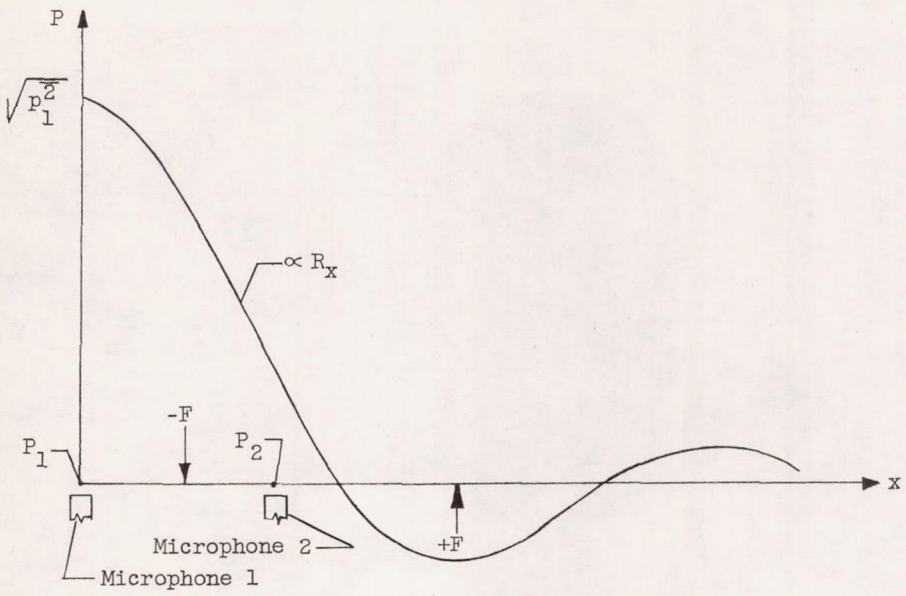

(a) Determined from measurements of R_x.

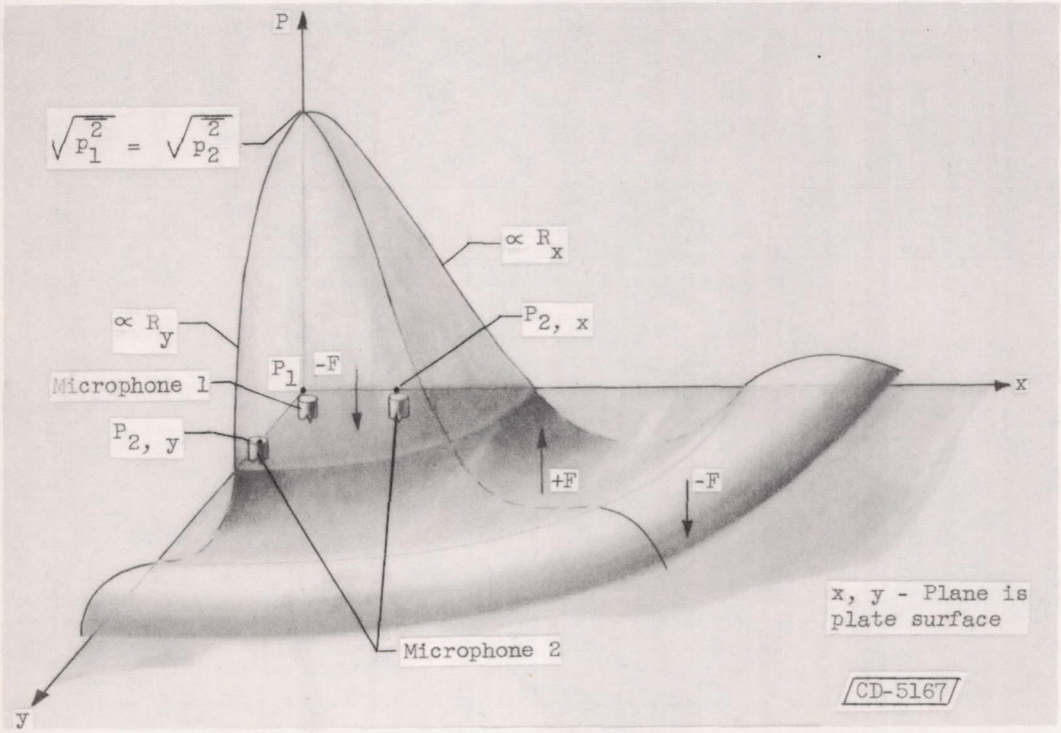

(b) Determined from measurements of R_x or R_y.

Figure 2. - Steady-state pressure distributions indicated by correlation measurements. Arrow with F indicates instantaneous direction of applied force.

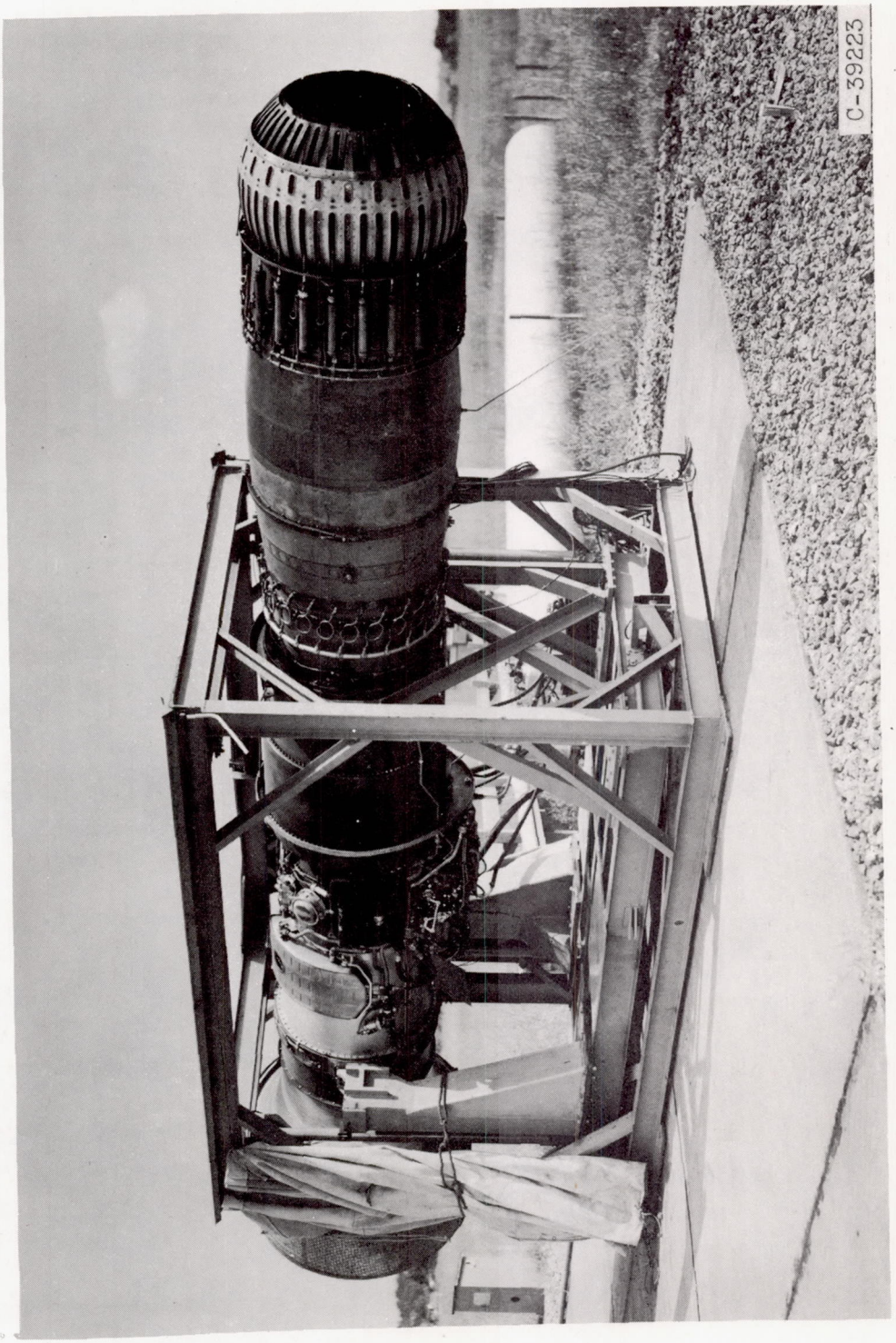

Figure 3. - Engine and thrust stand.

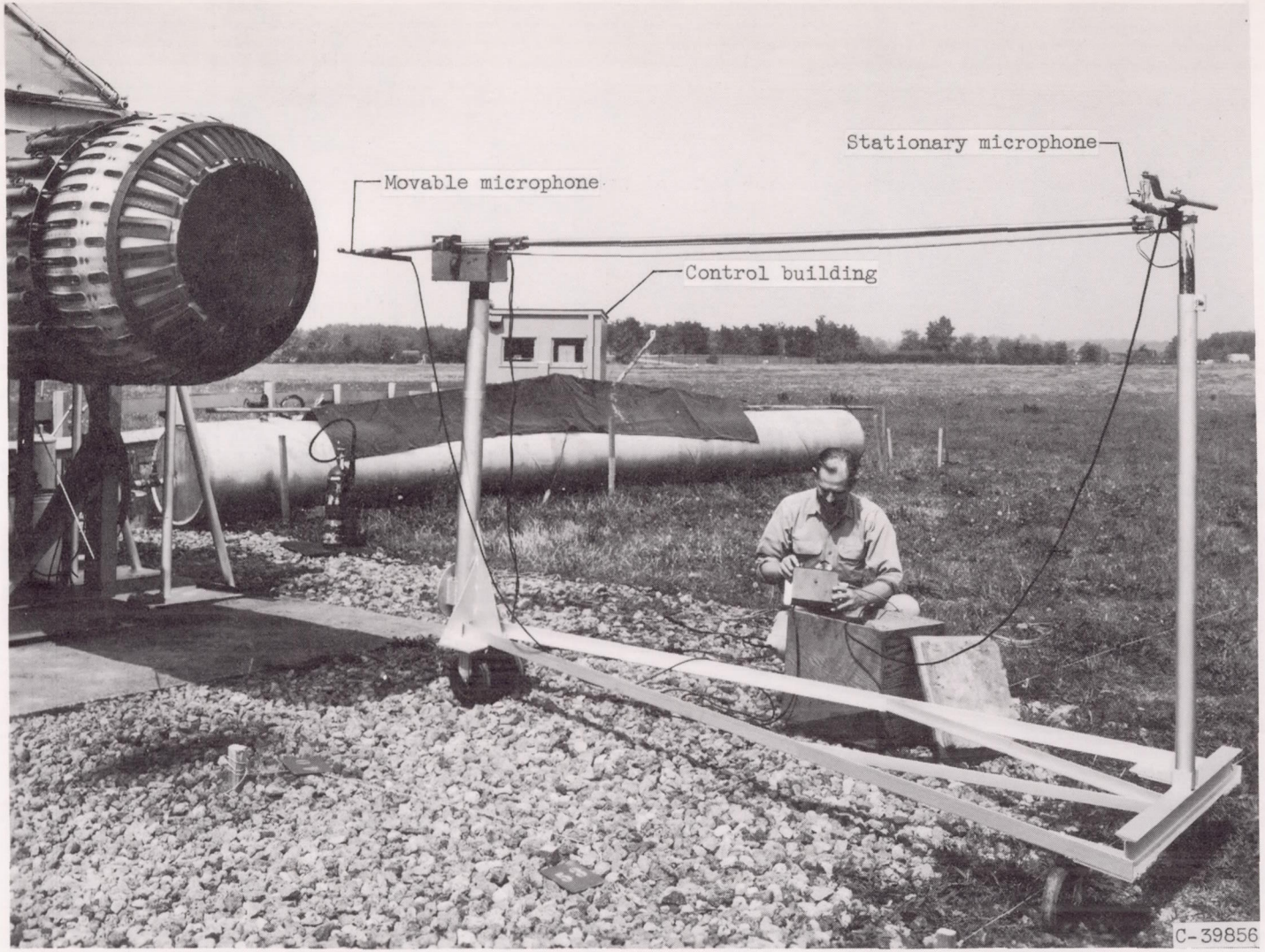

Figure 4. - Microphones and microphone positioner.

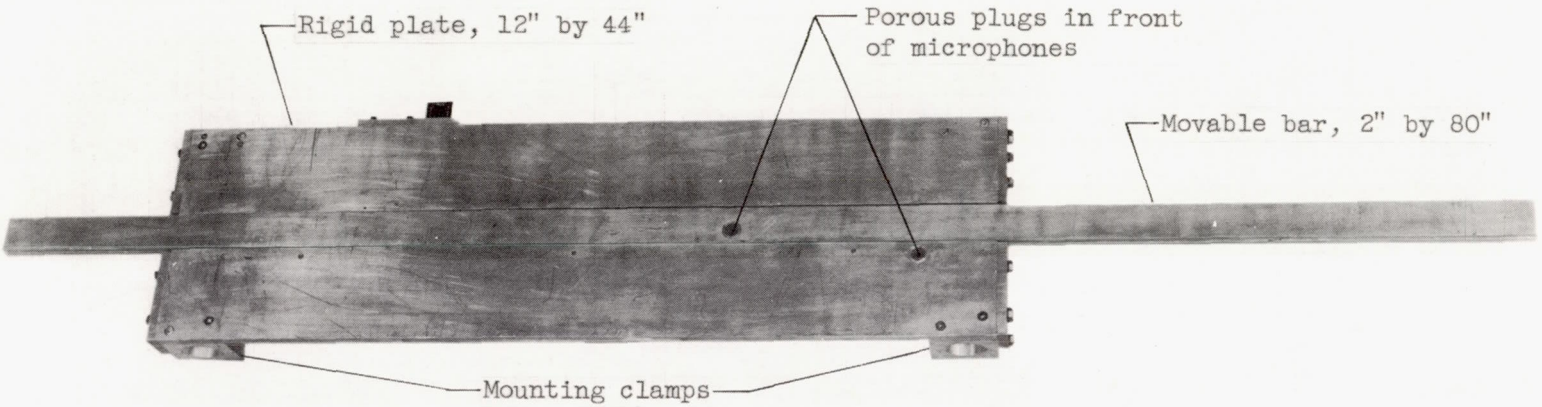

Figure 5. - Plate used for determining sound-pressure correlation on surface.

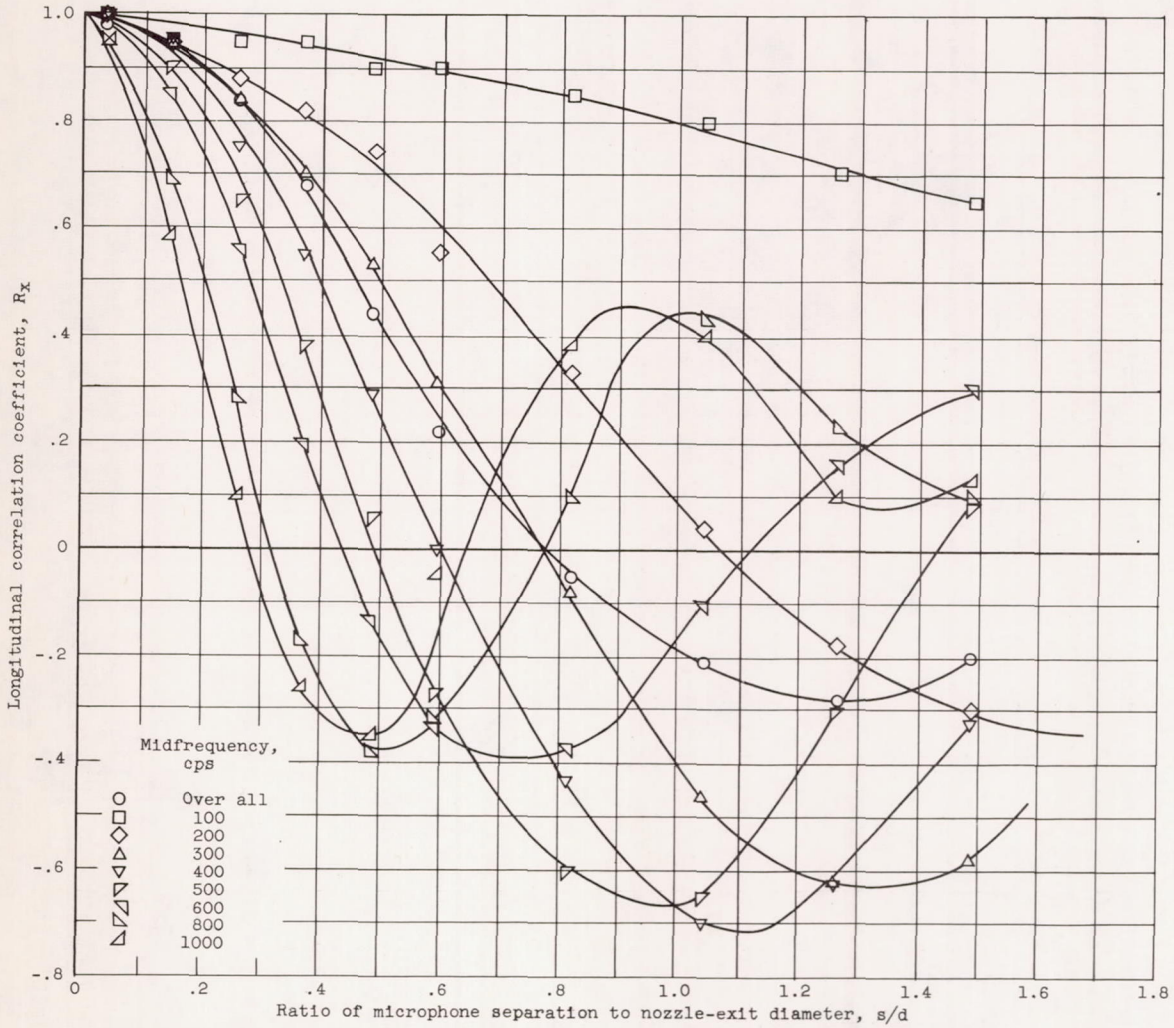

Figure 6. - Longitudinal sound-pressure correlation in various frequency bands. Distance downstream of nozzle exit x_1, 17.3 nozzle-exit diameters; distance from jet centerline z, 12.1 nozzle-exit diameters.

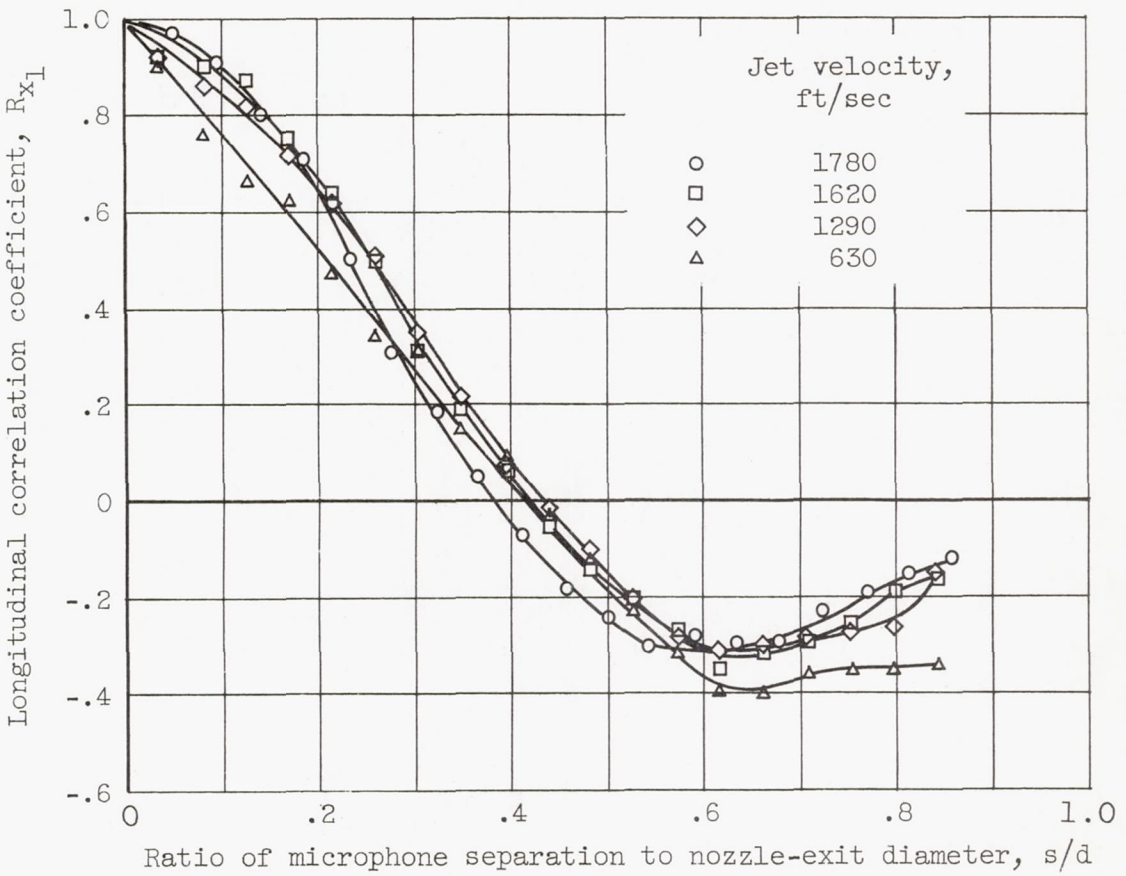

Figure 7. - Longitudinal correlation along jet boundary of over-all sound pressure for range of jet velocities. Distance downstream of nozzle exit x_1, 2.16 nozzle-exit diameters.

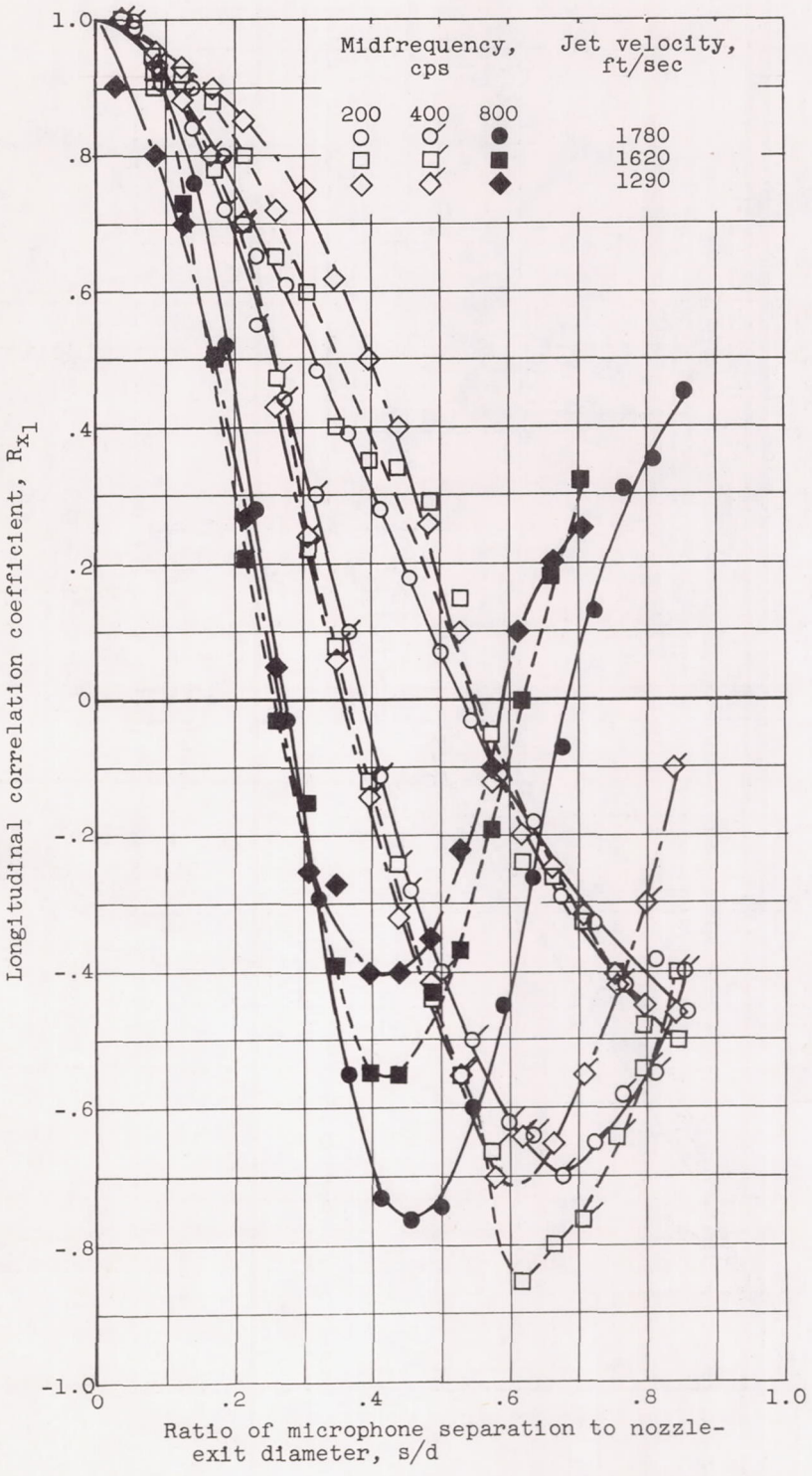

Figure 8. - Longitudinal correlation of sound pressure for three frequency bands. Distance downstream of nozzle exit x_1, 2.16 nozzle-exit diameters.

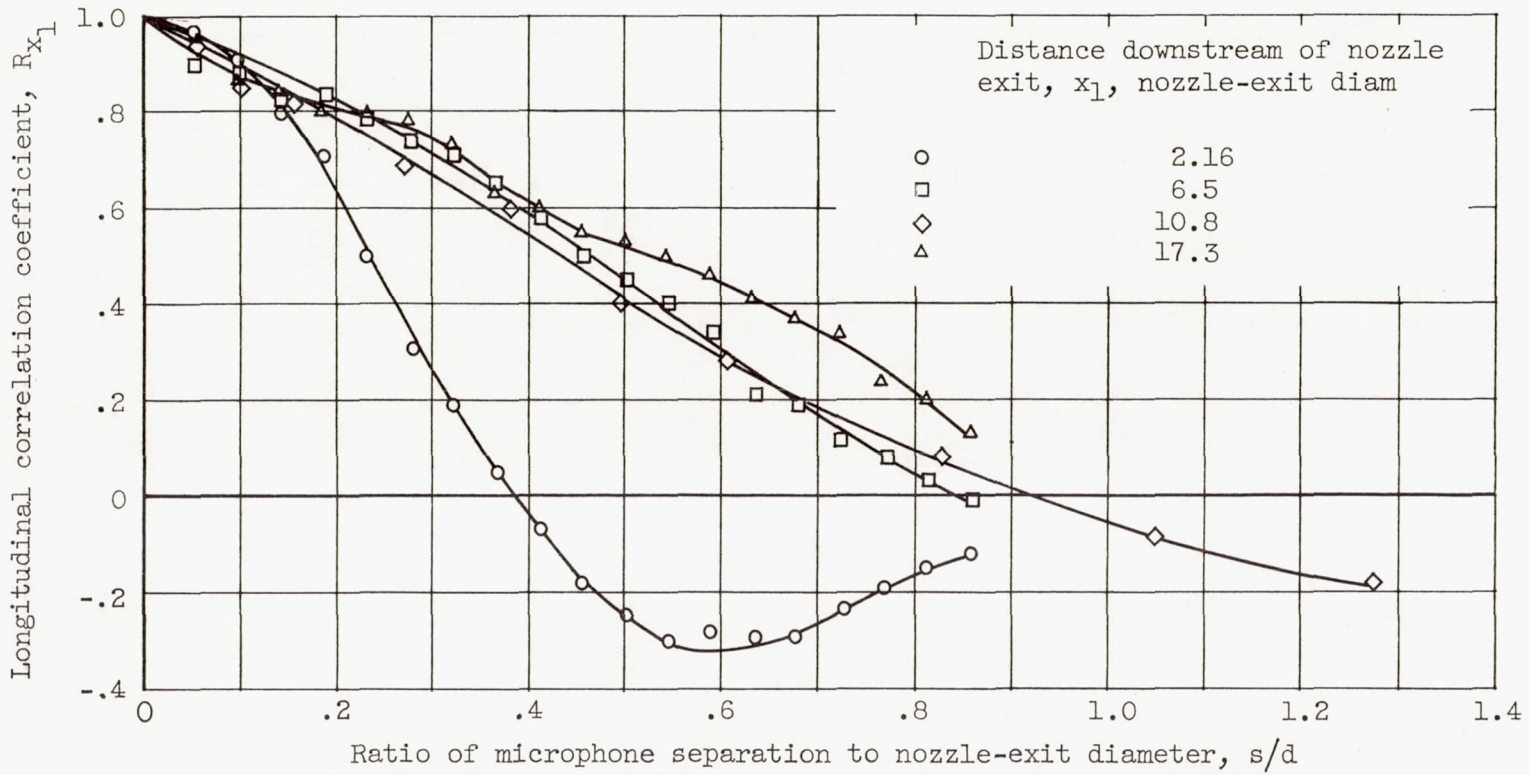

Figure 9. - Longitudinal correlation of over-all sound pressure at several locations along the jet boundary.

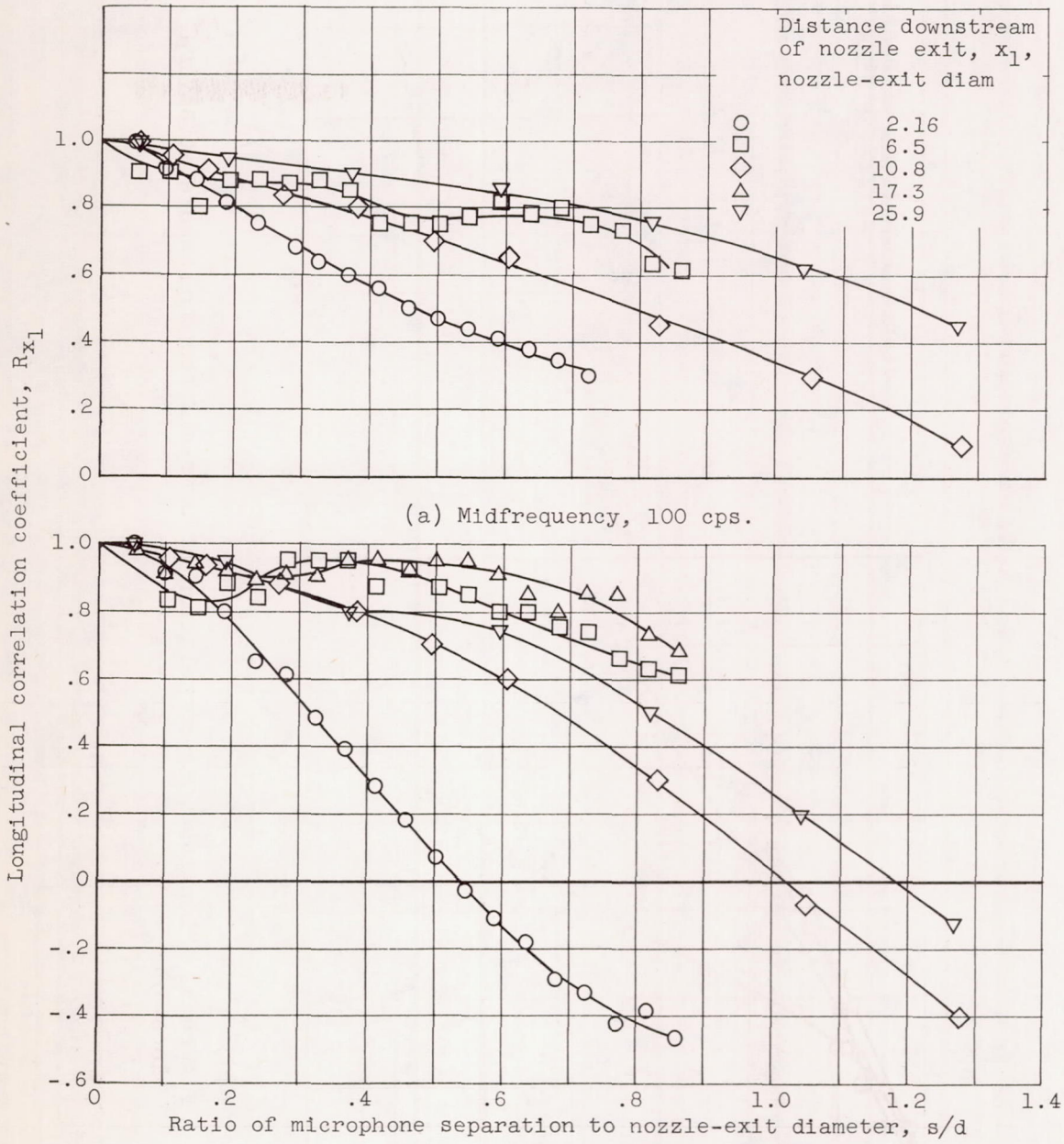

(a) Midfrequency, 100 cps.

(b) Midfrequency, 200 cps.

Figure 10. - Longitudinal correlation of sound pressure in various frequency bands for several positions along the jet boundary.

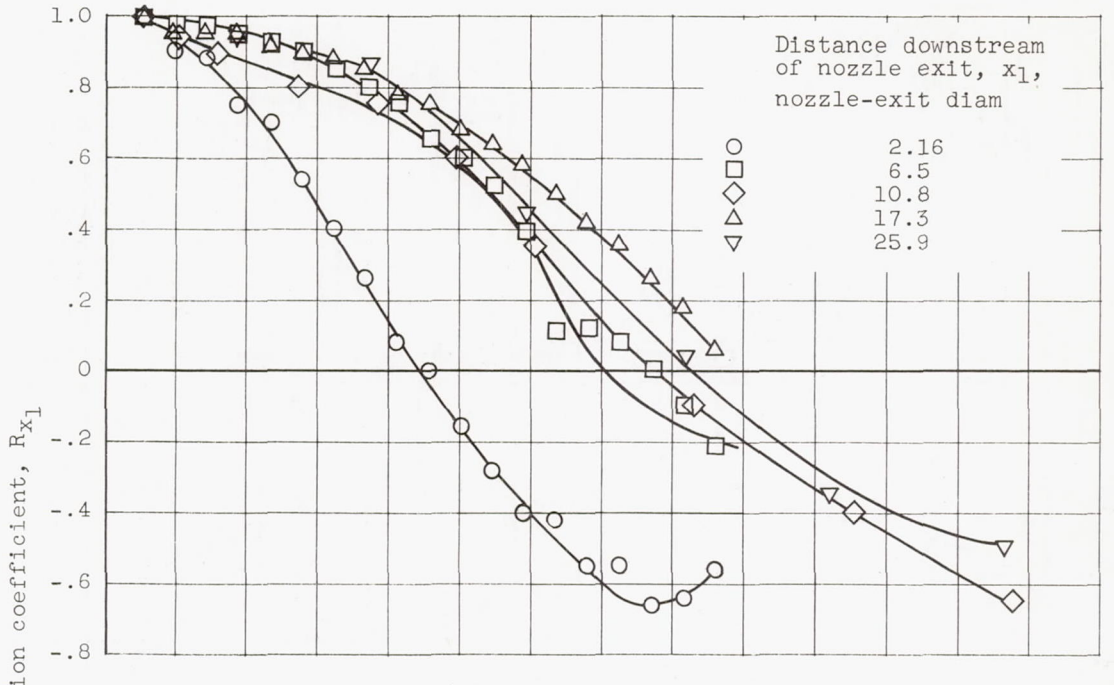

(c) Midfrequency, 300 cps.

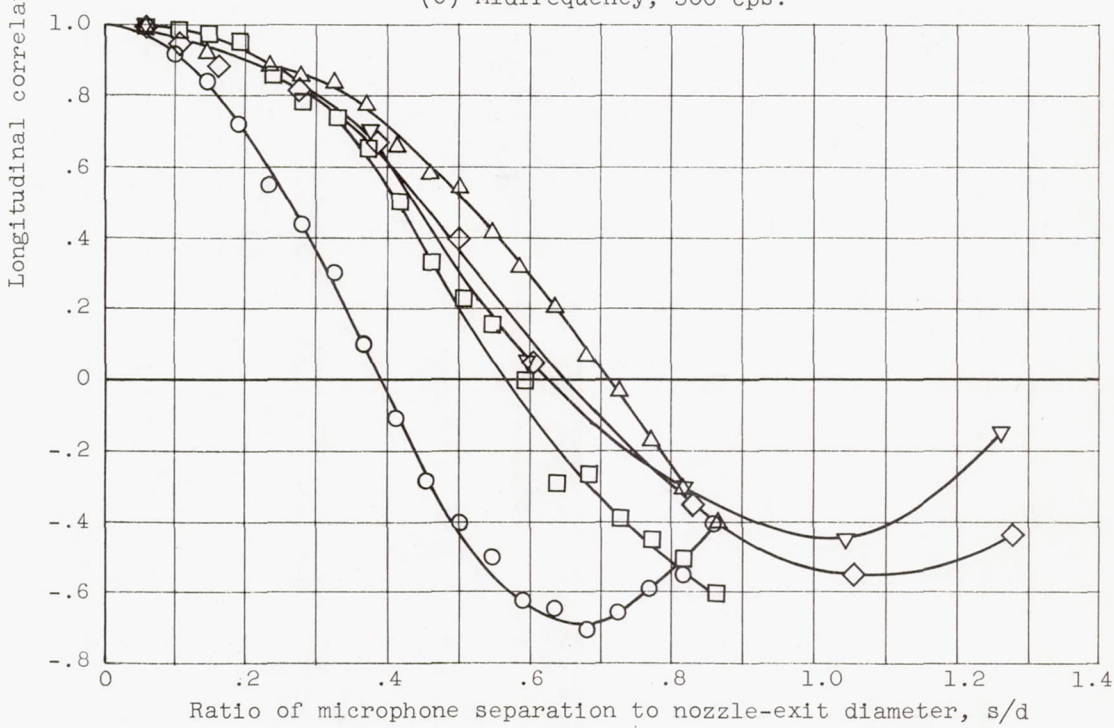

(d) Midfrequency, 400 cps.

Figure 10. - Continued. Longitudinal correlation of sound pressure in various frequency bands for several positions along the jet boundary.

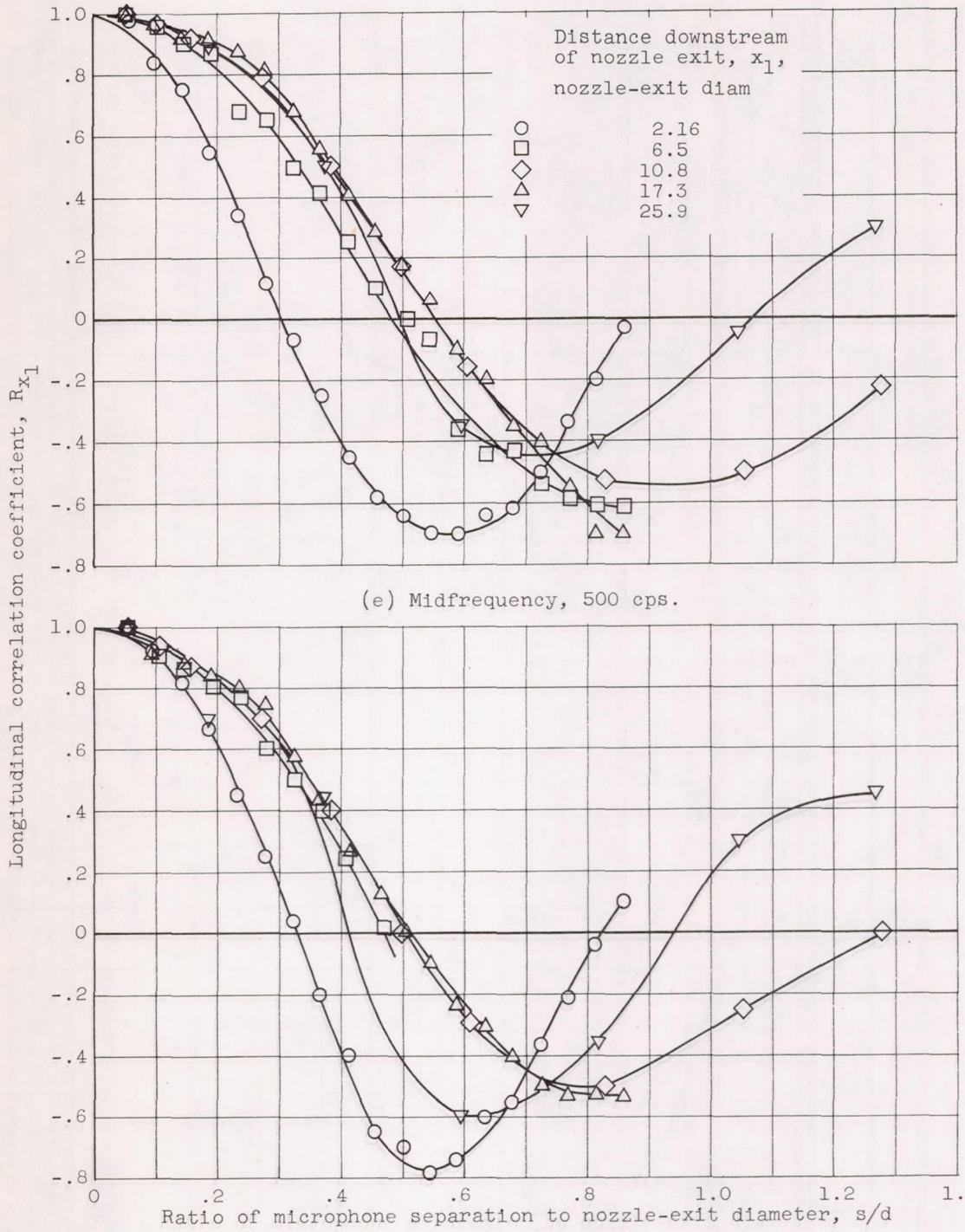

(e) Midfrequency, 500 cps.

(f) Midfrequency, 600 cps.

Figure 10. - Continued. Longitudinal correlation of sound pressure in various frequency bands for several positions along the jet boundary.

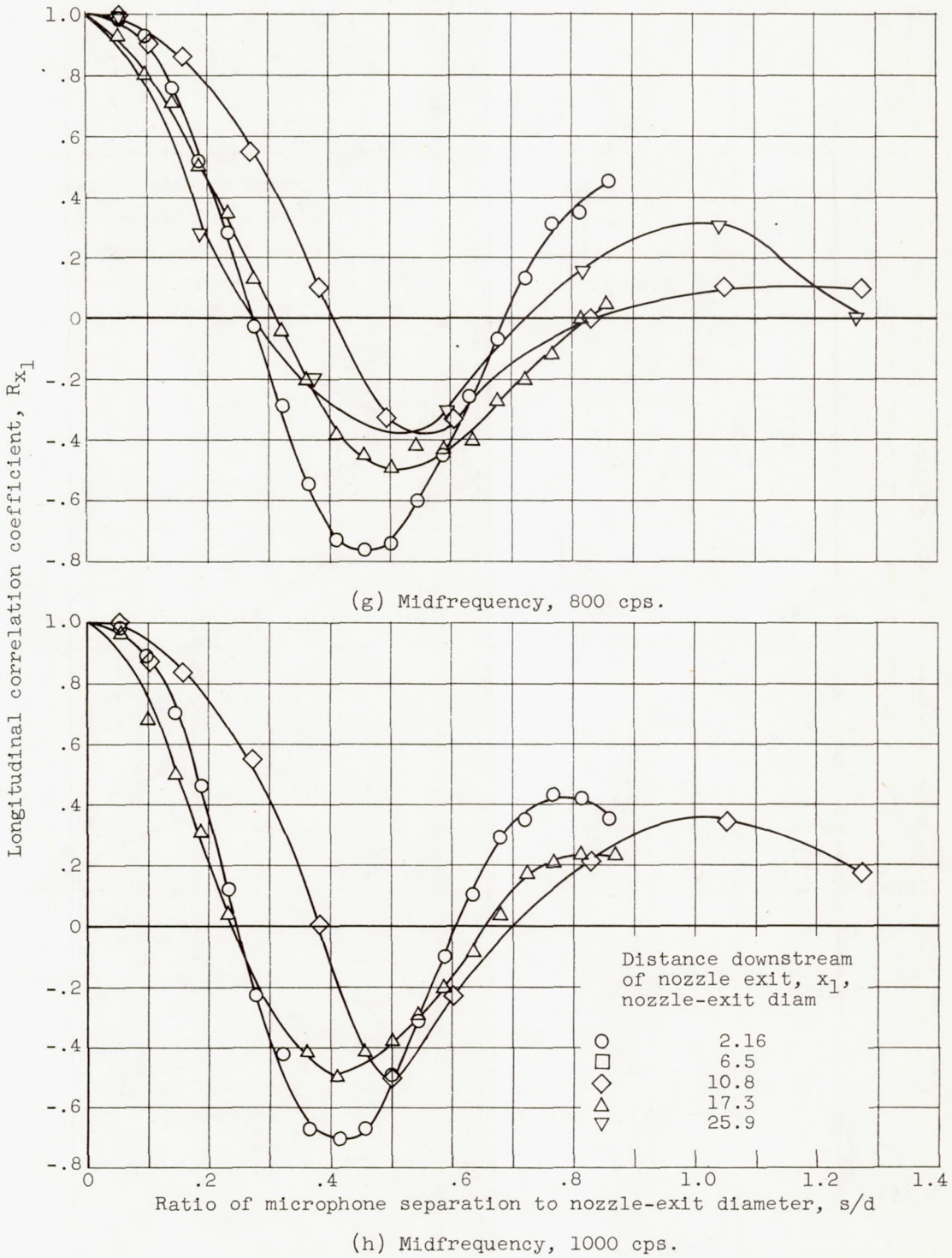

(g) Midfrequency, 800 cps.

(h) Midfrequency, 1000 cps.

Figure 10. - Concluded. Longitudinal correlation of sound pressure in various frequency bands for several positions along the jet boundary.

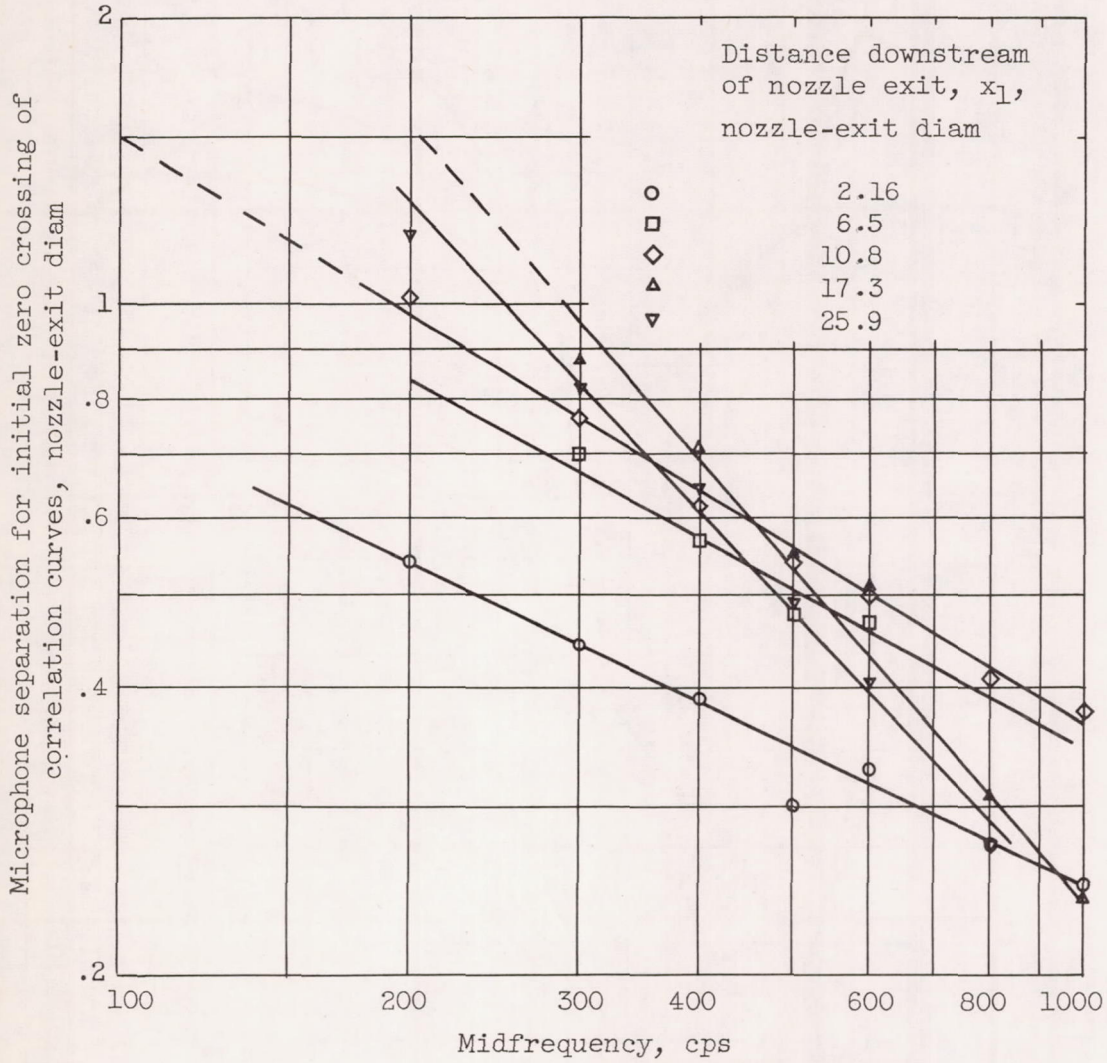

Figure 11. - Initial zero crossing of longitudinal correlation curves as function of frequency.

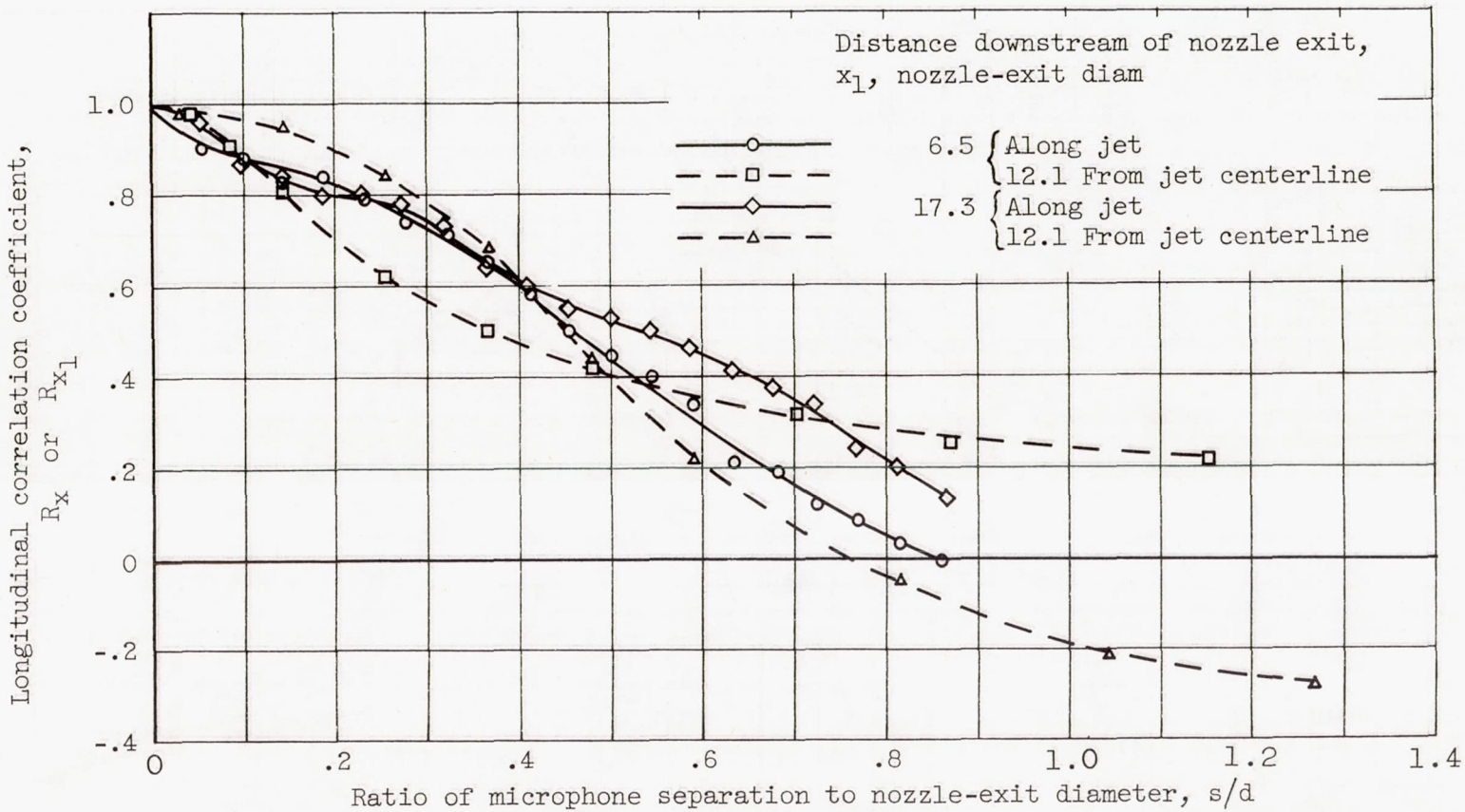

Figure 12. - Longitudinal correlations of over-all sound pressure along jet boundary and 12.1 nozzle-exit diameters from jet centerline for two distances downstream of nozzle exit.

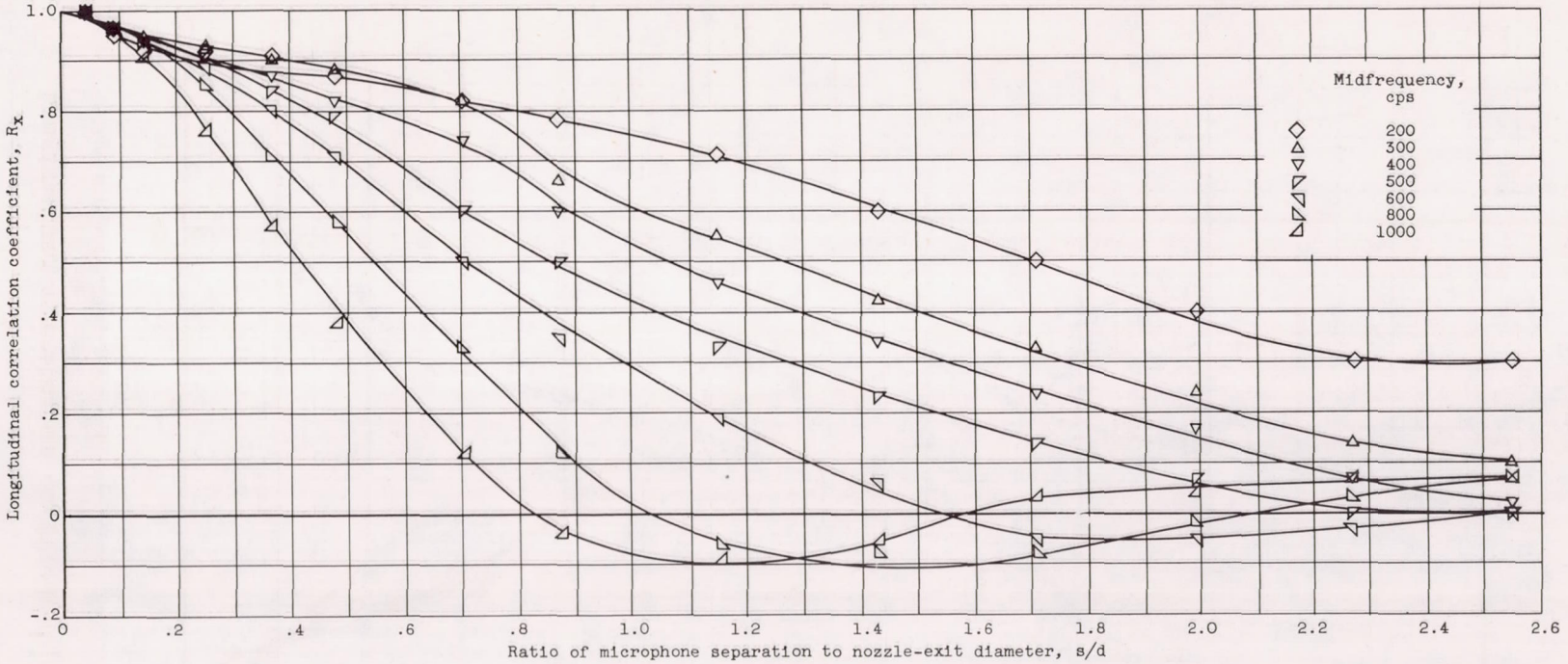

Figure 13. - Longitudinal correlation of sound pressure for several frequency bands. Distance downstream of nozzle exit x_1, 6.5 nozzle-exit diameters; distance from jet centerline z, 12.1 nozzle-exit diameters.

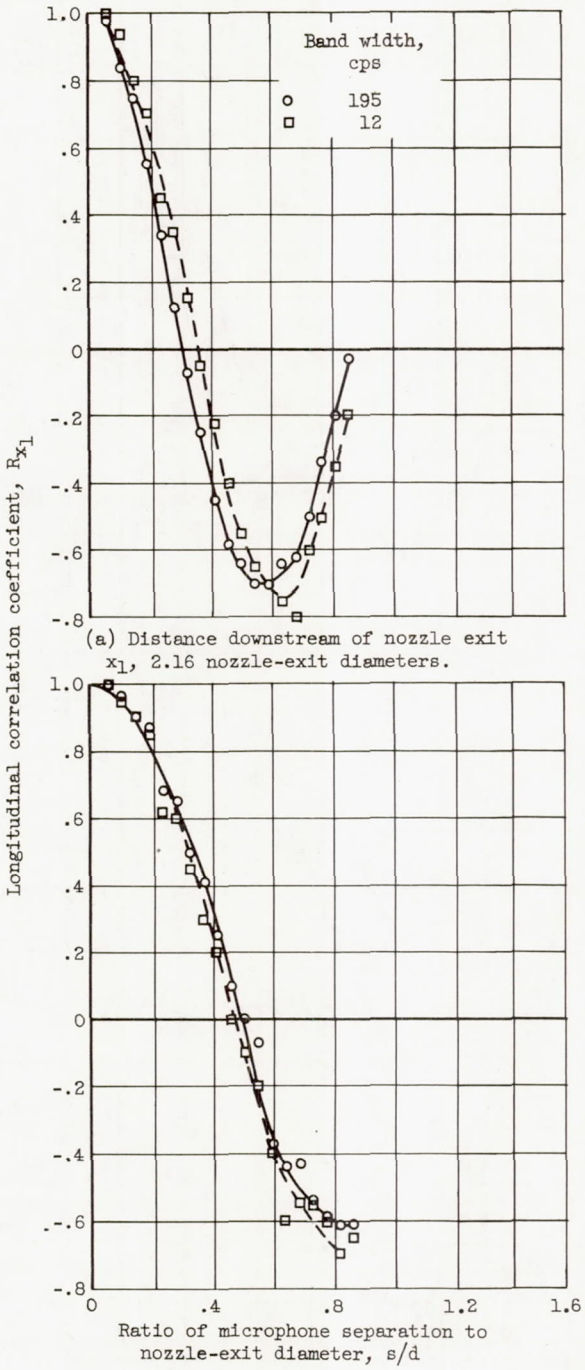

(a) Distance downstream of nozzle exit x_1, 2.16 nozzle-exit diameters.

(b) Distance downstream of nozzle exit x_1, 6.5 nozzle-exit diameters.

Figure 14. - Longitudinal correlations of sound pressure for two band widths having midfrequencies of 500 cps.

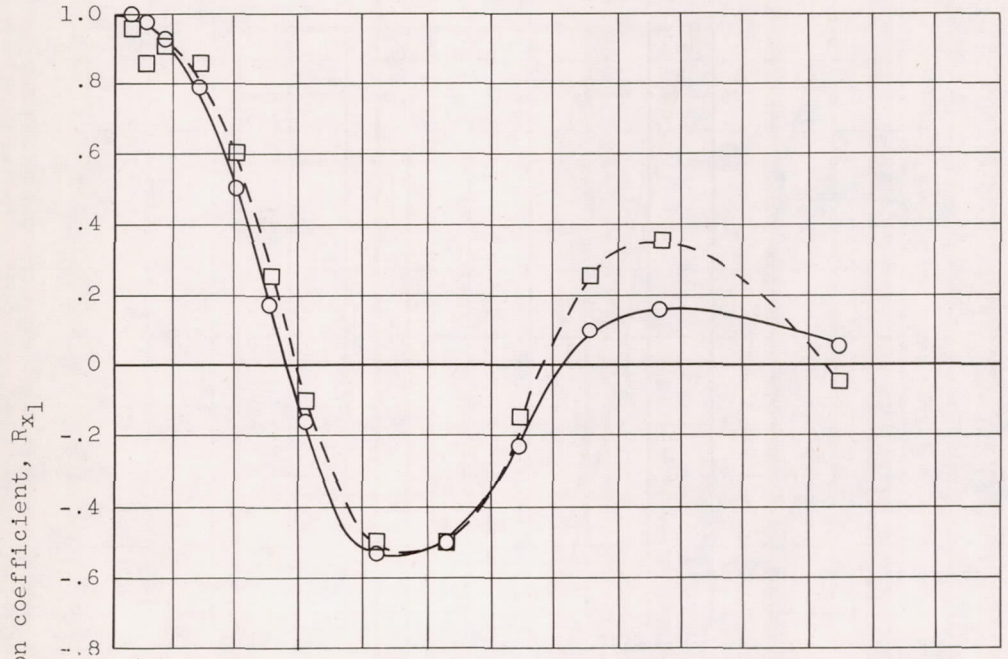

(c) Distance downstream of nozzle exit x_1, 10.8 nozzle-exit diameters.

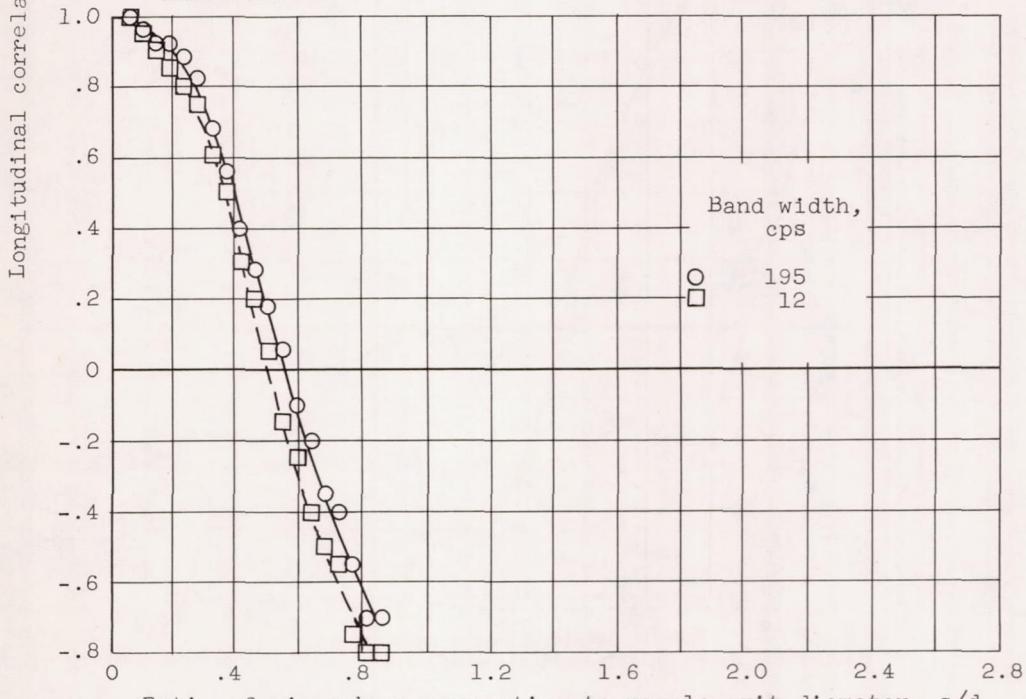

(d) Distance downstream of nozzle exit x_1, 17.3 nozzle-exit diameters.

Figure 14. - Continued. Longitudinal correlations of sound pressure for two band widths having midfrequencies of 500 cps.

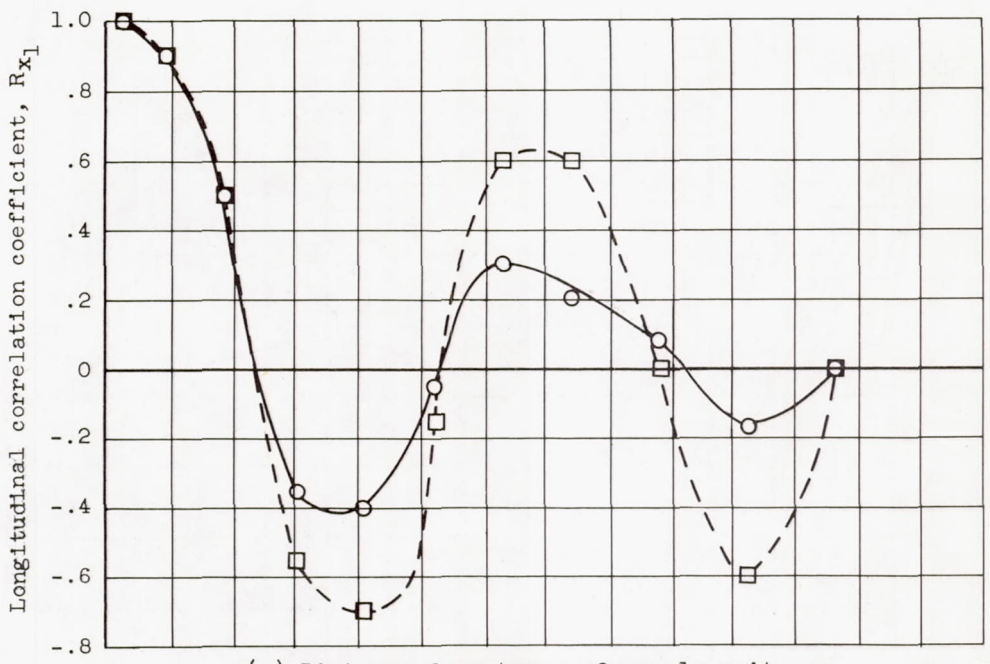

(e) Distance downstream of nozzle exit x_1, 25.9 nozzle-exit diameters.

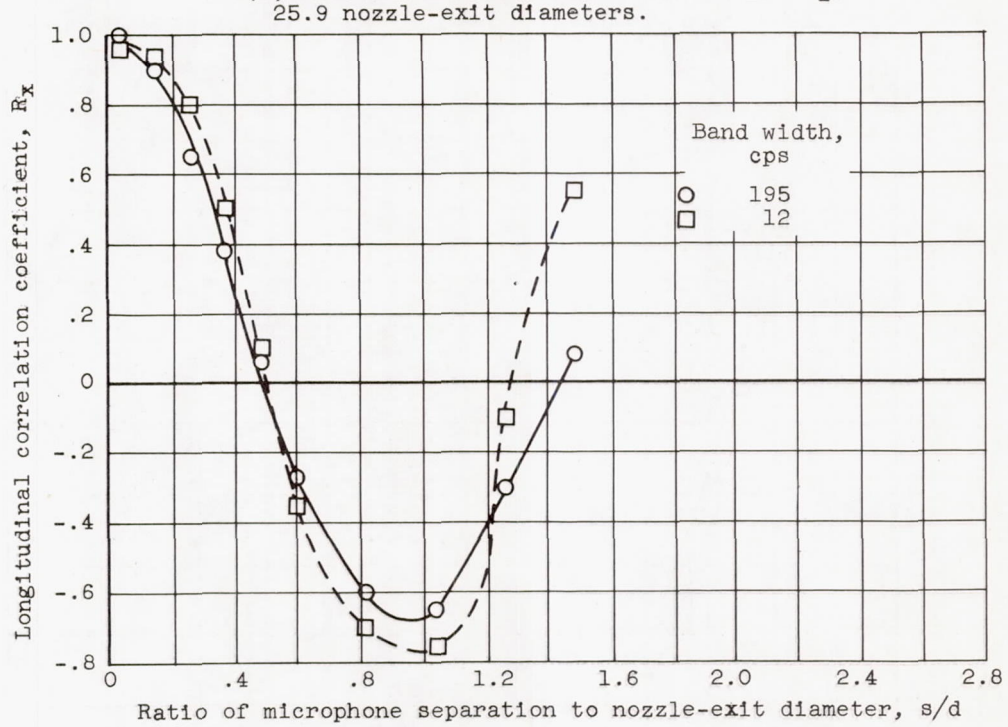

(f) Distance downstream of nozzle exit x_1, 17.3 nozzle-exit diameters; distance from jet centerline z, 12.1 nozzle-exit diameters.

Figure 14. - Concluded. Longitudinal correlations of sound pressure for two band widths having midfrequencies of 500 cps.

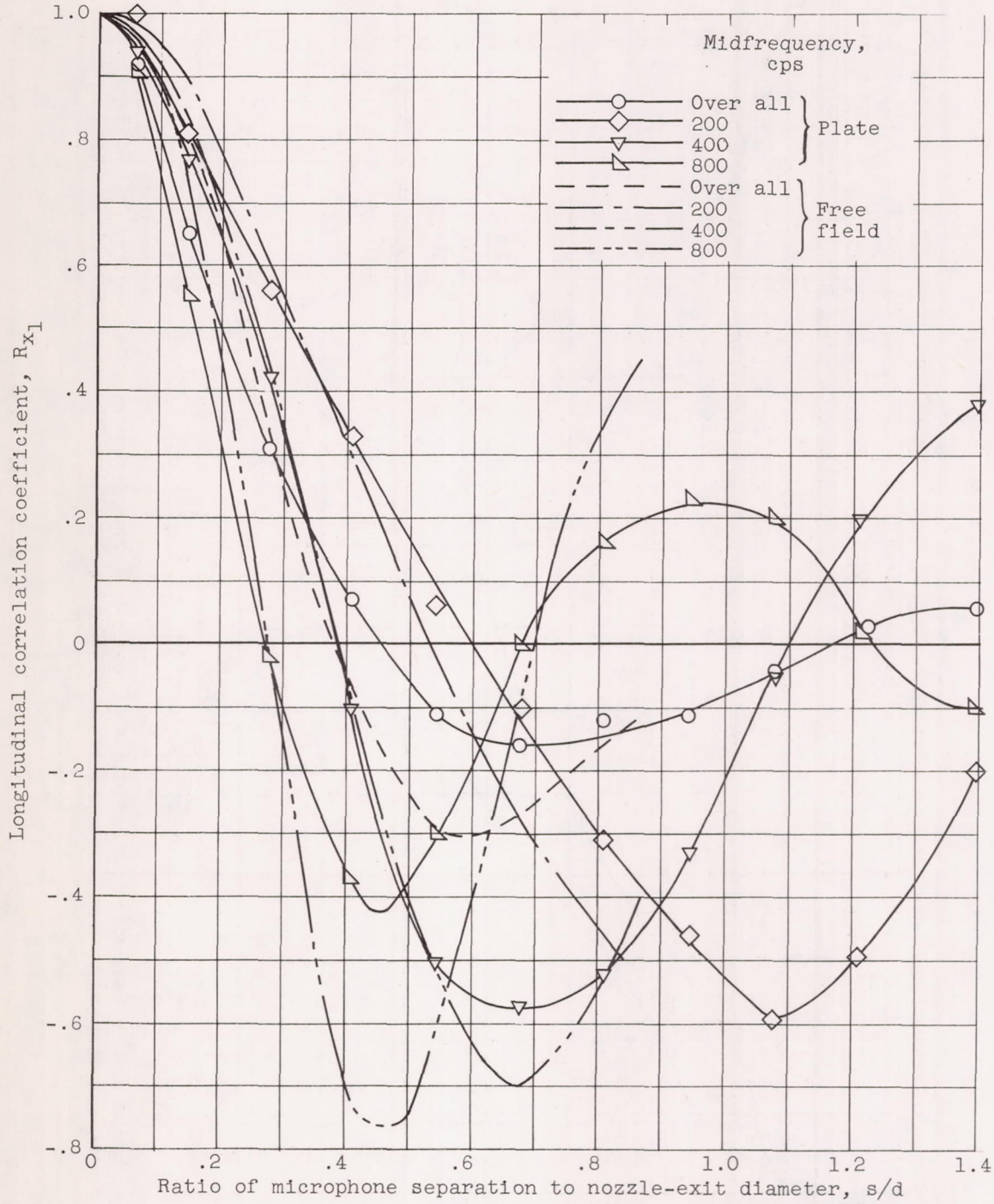

Figure 15. - Comparison of longitudinal correlations along jet boundary obtained on plate and in free field for several frequency bands. Fixed microphone, distance downstream of nozzle exit: plate x_1, 2.7 nozzle-exit diameters; free field x_1, 2.16 nozzle-exit diameters.

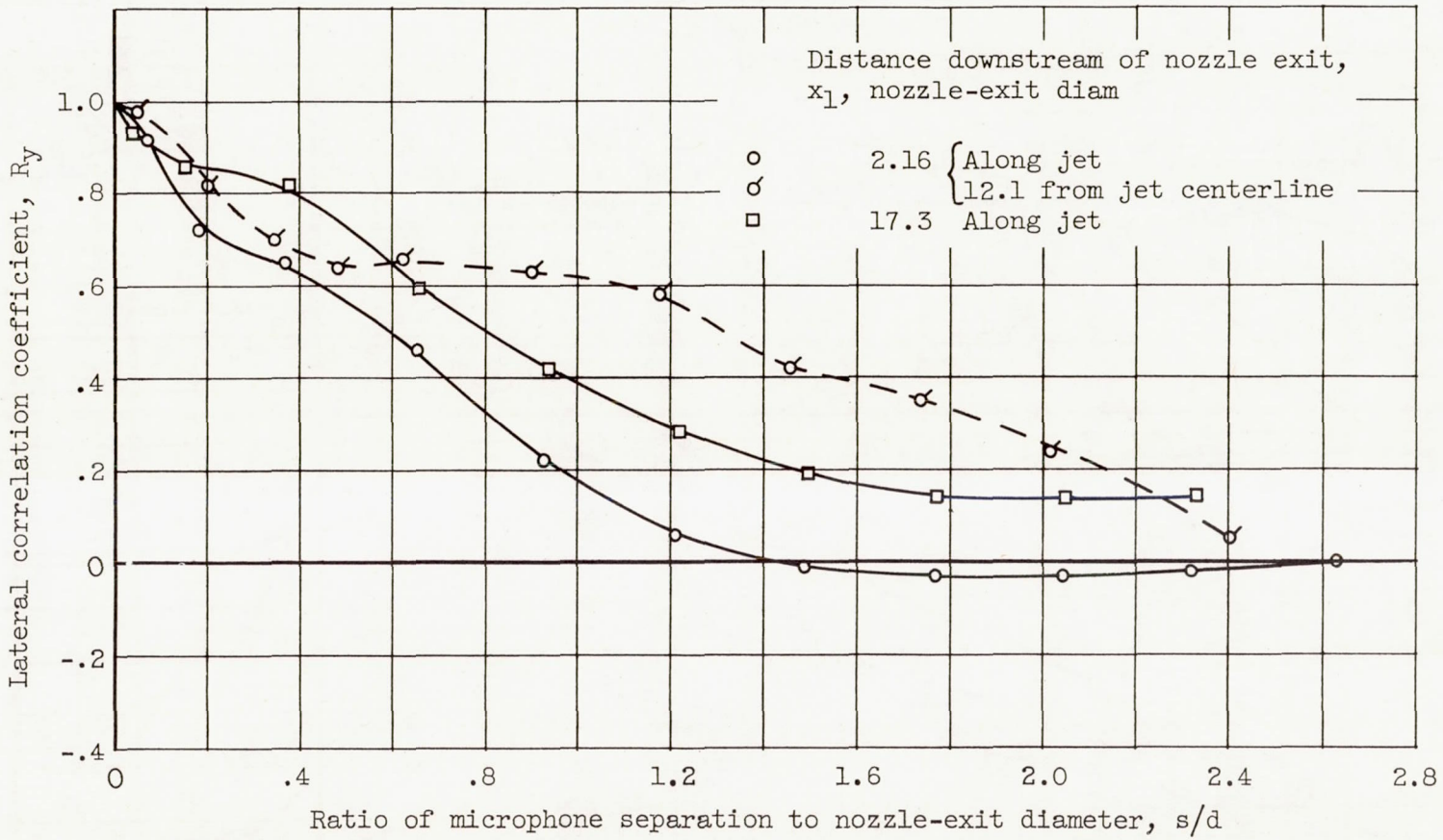

Figure 16. - Lateral correlations of over-all sound pressure at several locations in sound field.

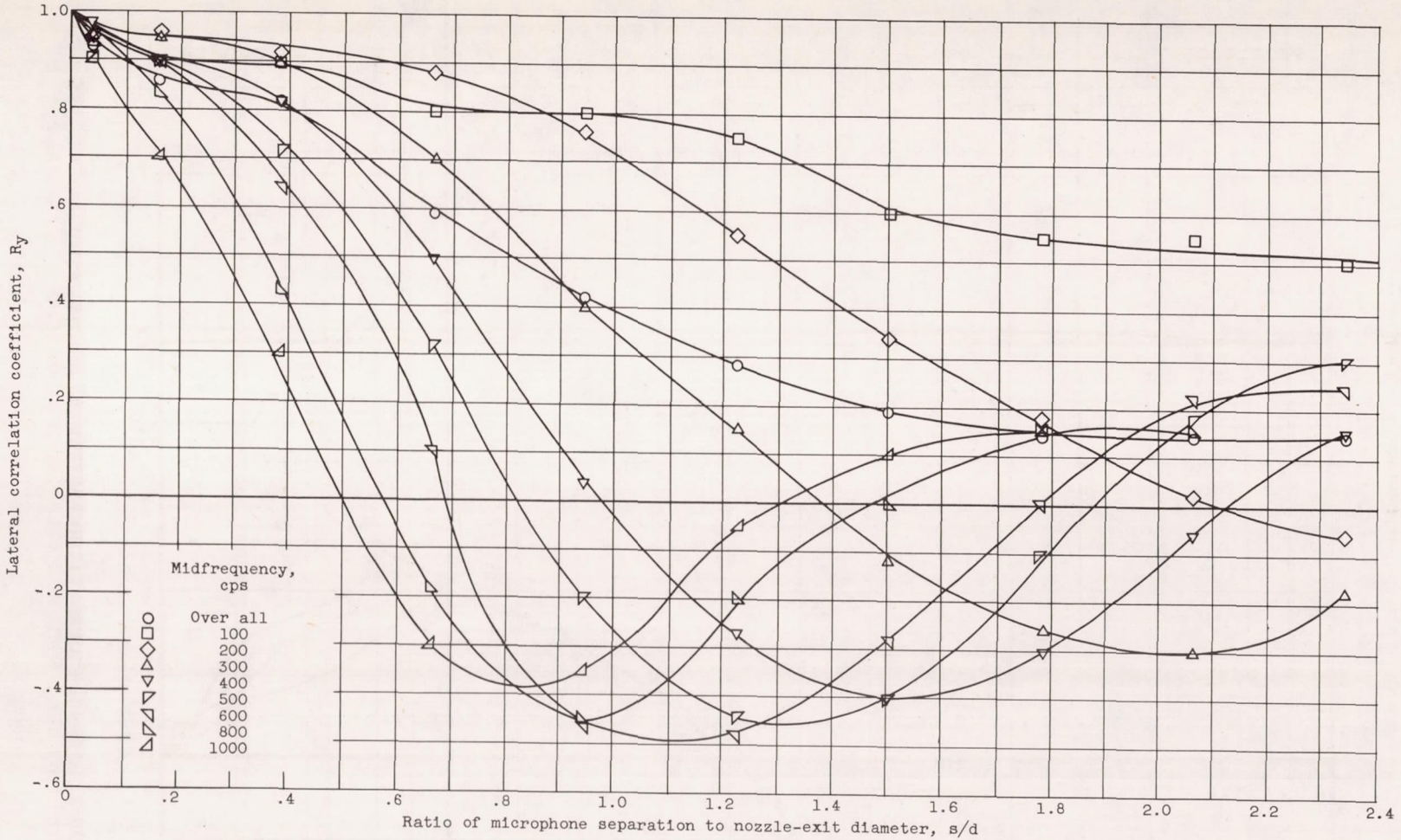

Figure 17. - Lateral correlation of sound pressure at jet boundary for various frequency bands. Distance downstream of nozzle exit x_1, 17.3 nozzle-exit diameters.

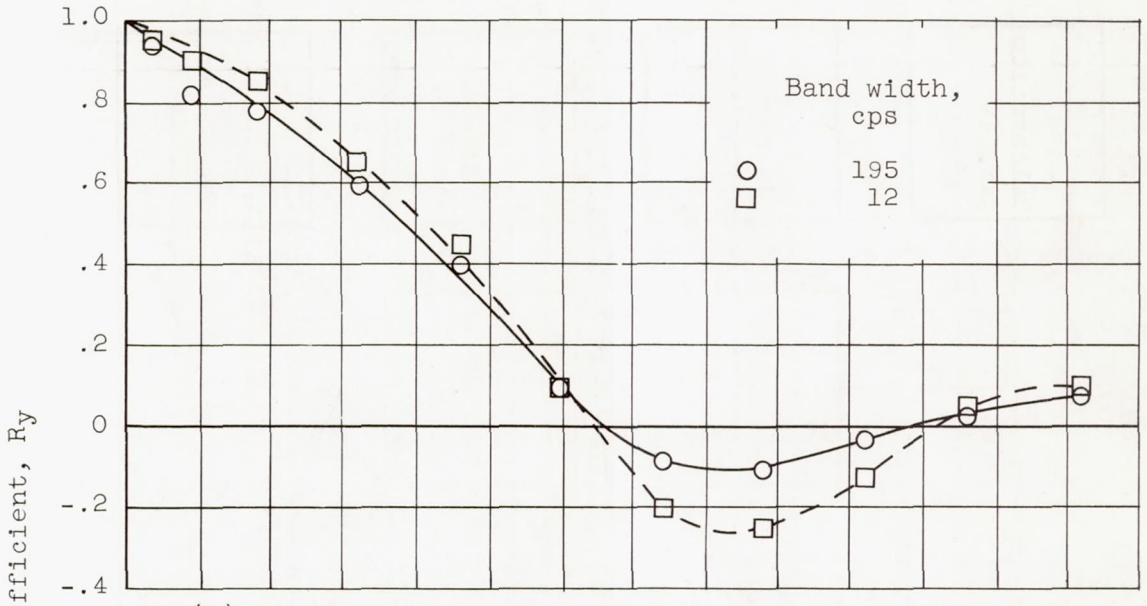

(a) Distance downstream of nozzle exit x_1, 2.16 nozzle-exit diameters.

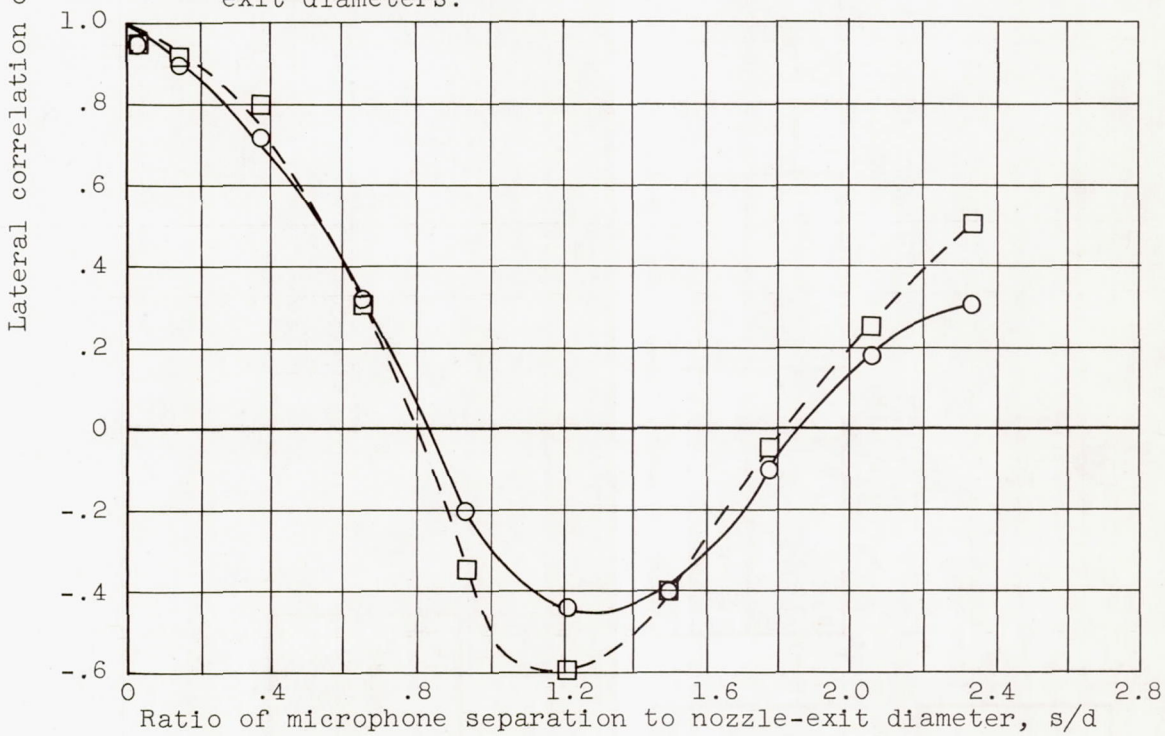

(b) Distance downstream of nozzle exit x_1, 17.3 nozzle-exit diameters.

Figure 18. - Lateral correlation of sound pressure at jet boundary for two band widths having midrequencies of 500 cps.

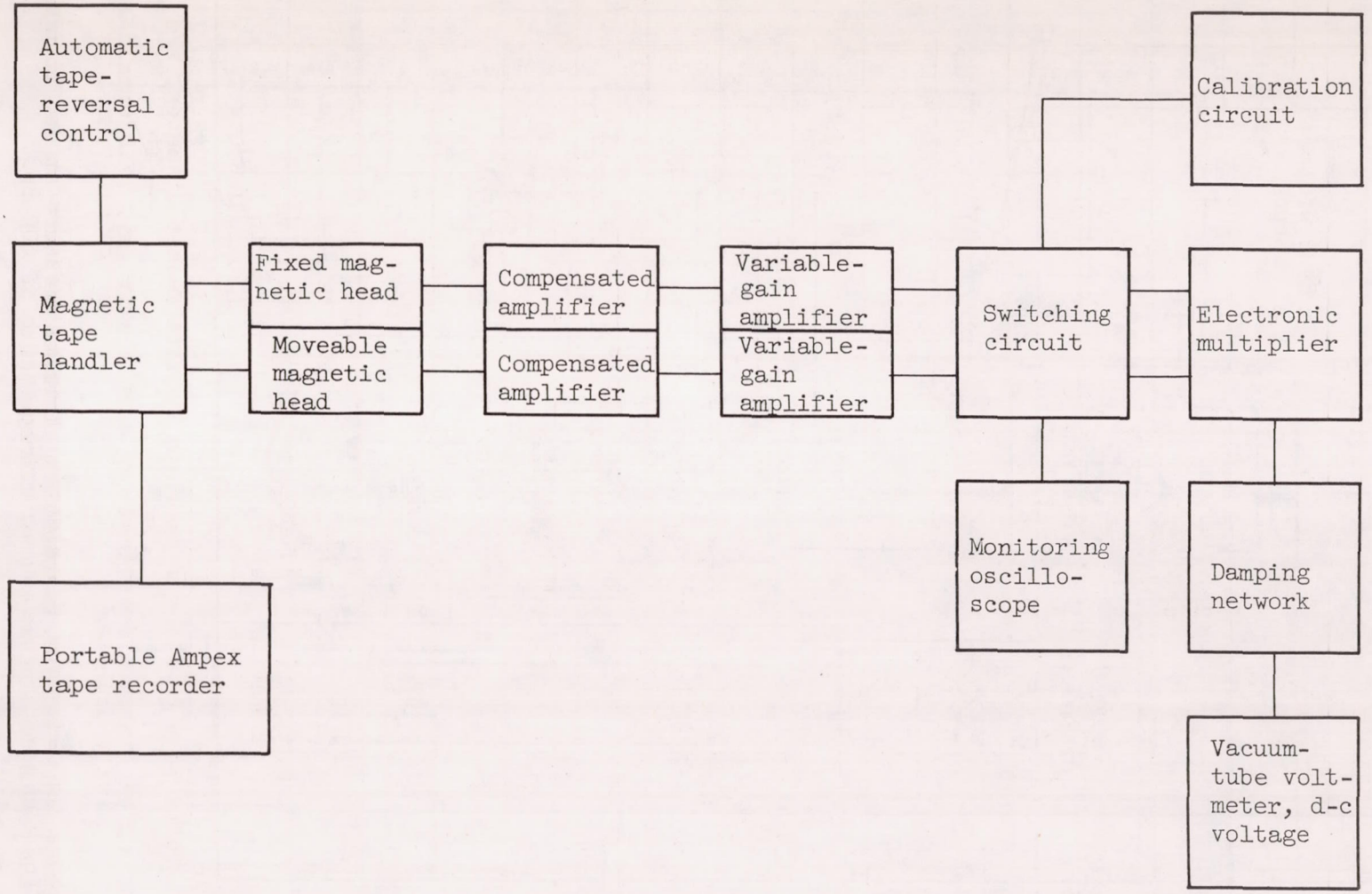

Figure 19. - Block diagram of correlation computer.

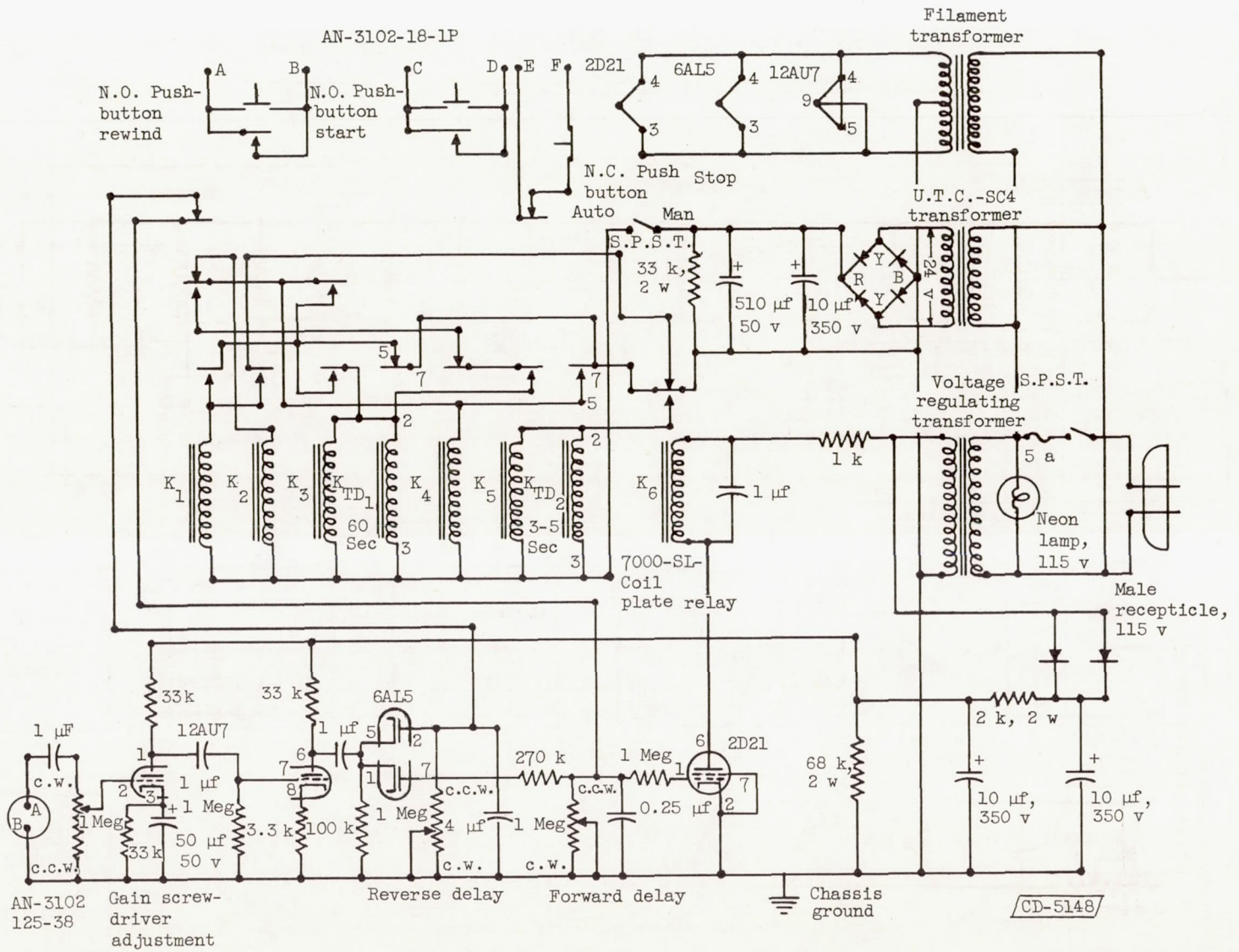

Figure 20. - Automatic tape-reversal mechanism.

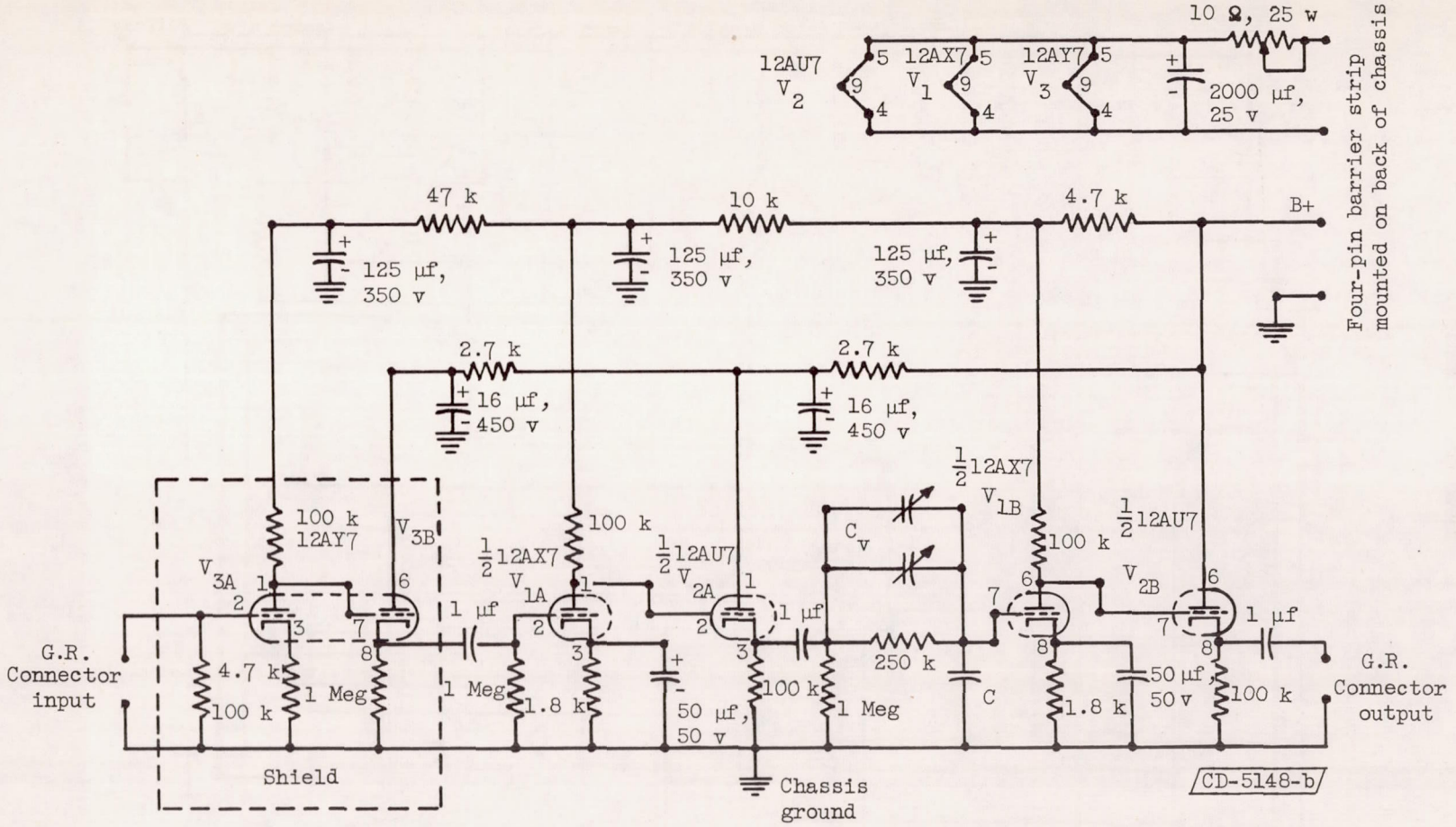

Figure 21. - Playback amplifier for correlation computer.

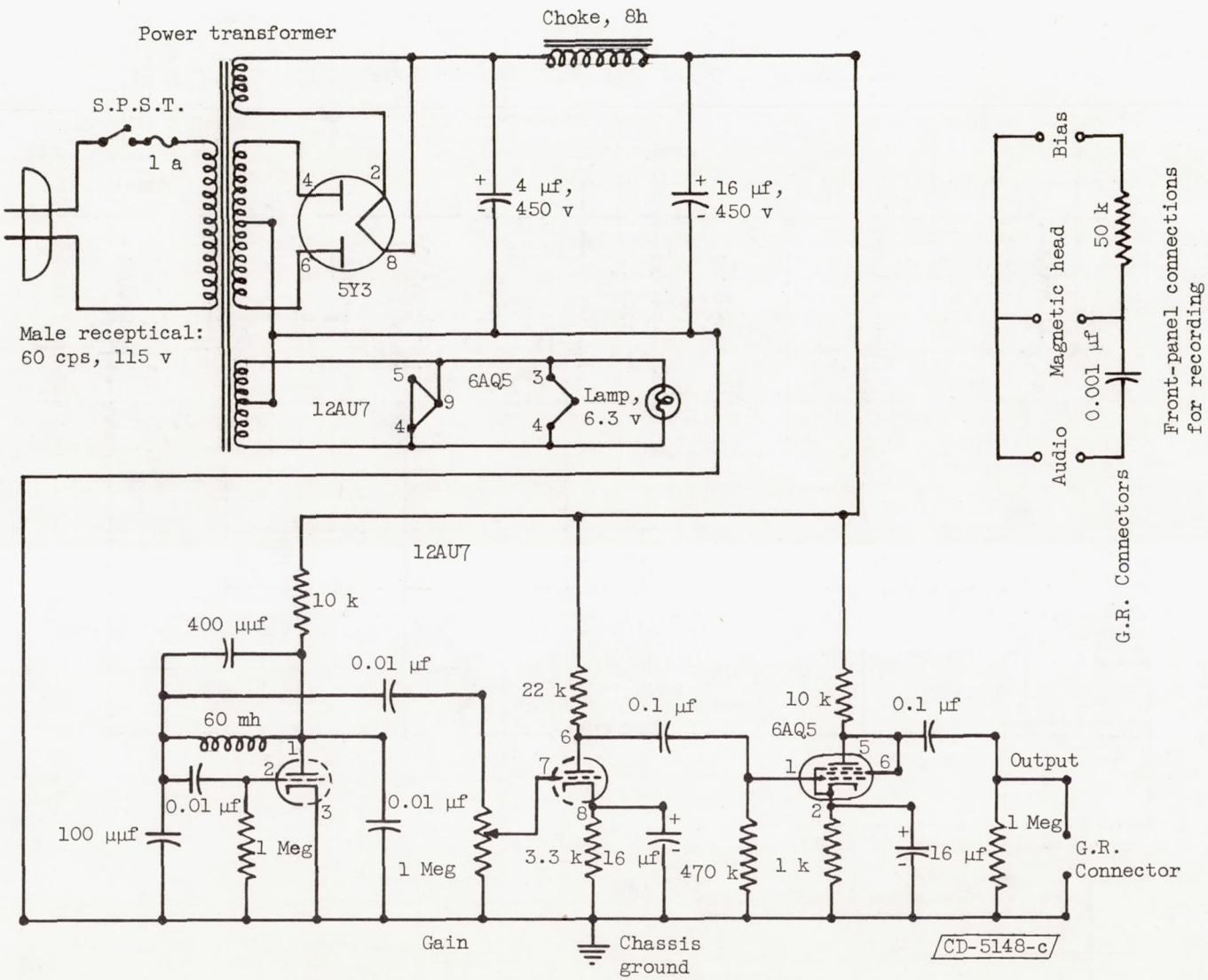

Figure 22. - Bias oscillator for recording.

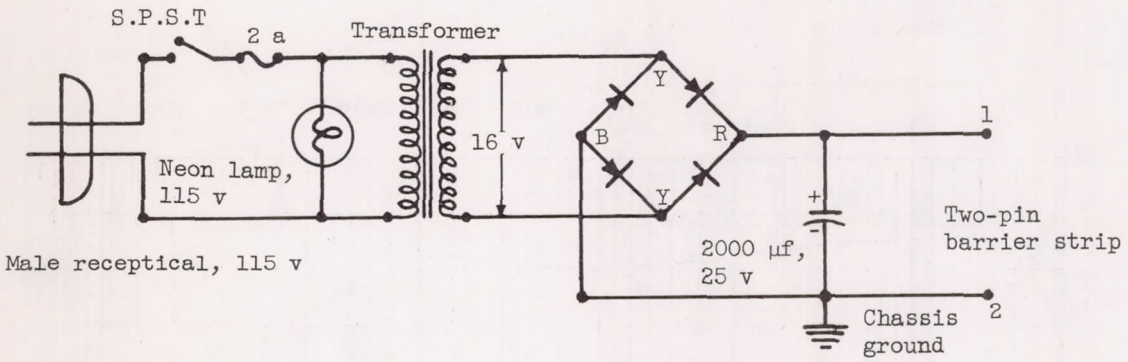

(a) Filament.

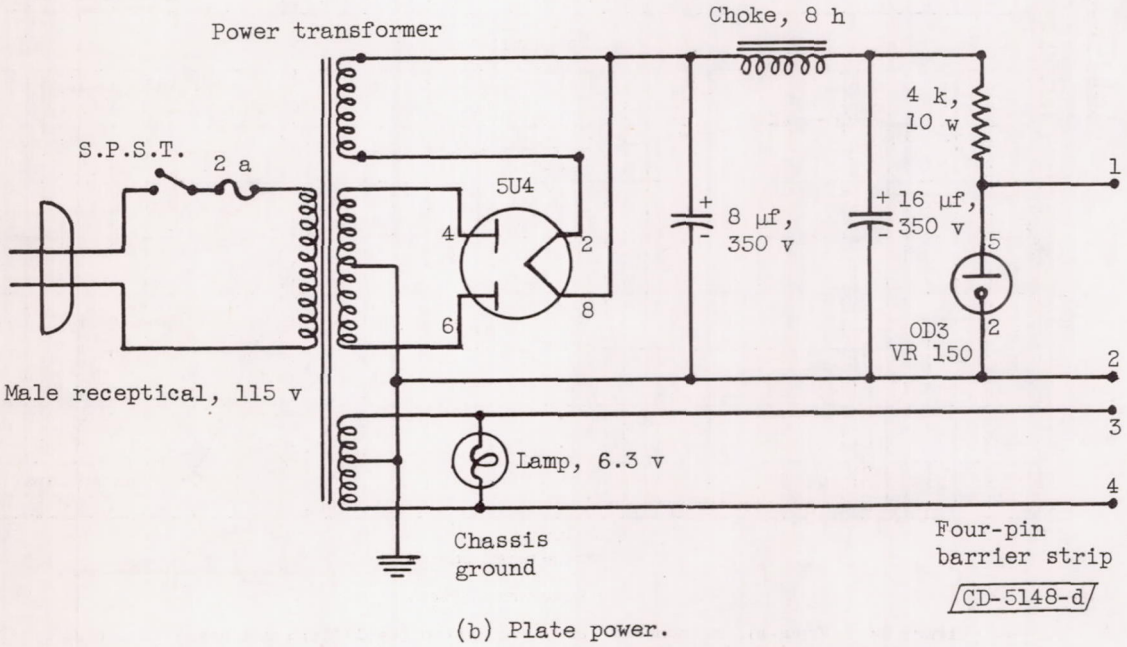

(b) Plate power.

Figure 23. - Voltage supply for playback amplifiers.

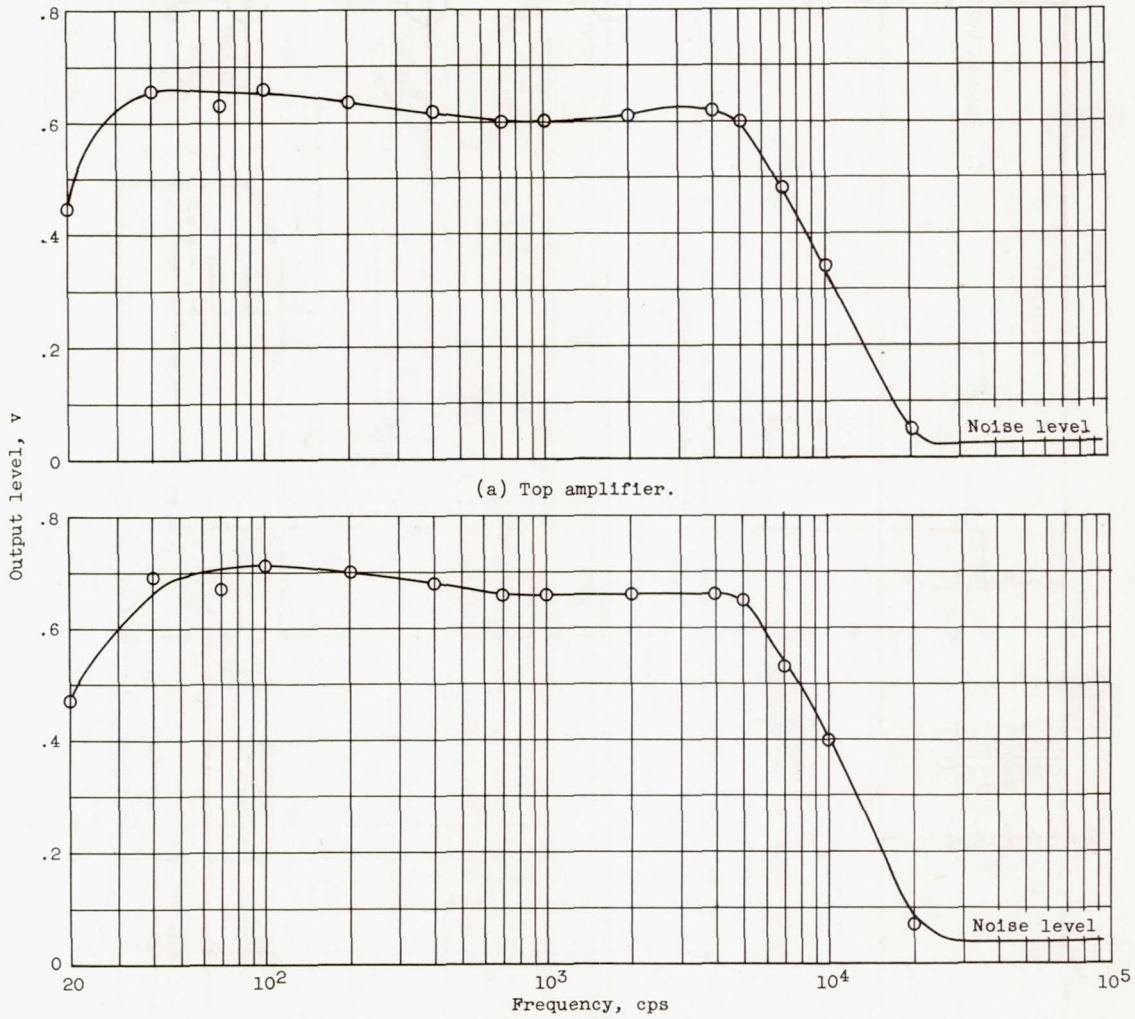

(a) Top amplifier.

(b) Lower amplifier.

Figure 24. - Over-all response of playback system (amplifiers and head) to a flat signal recorded on Ampex equipment.

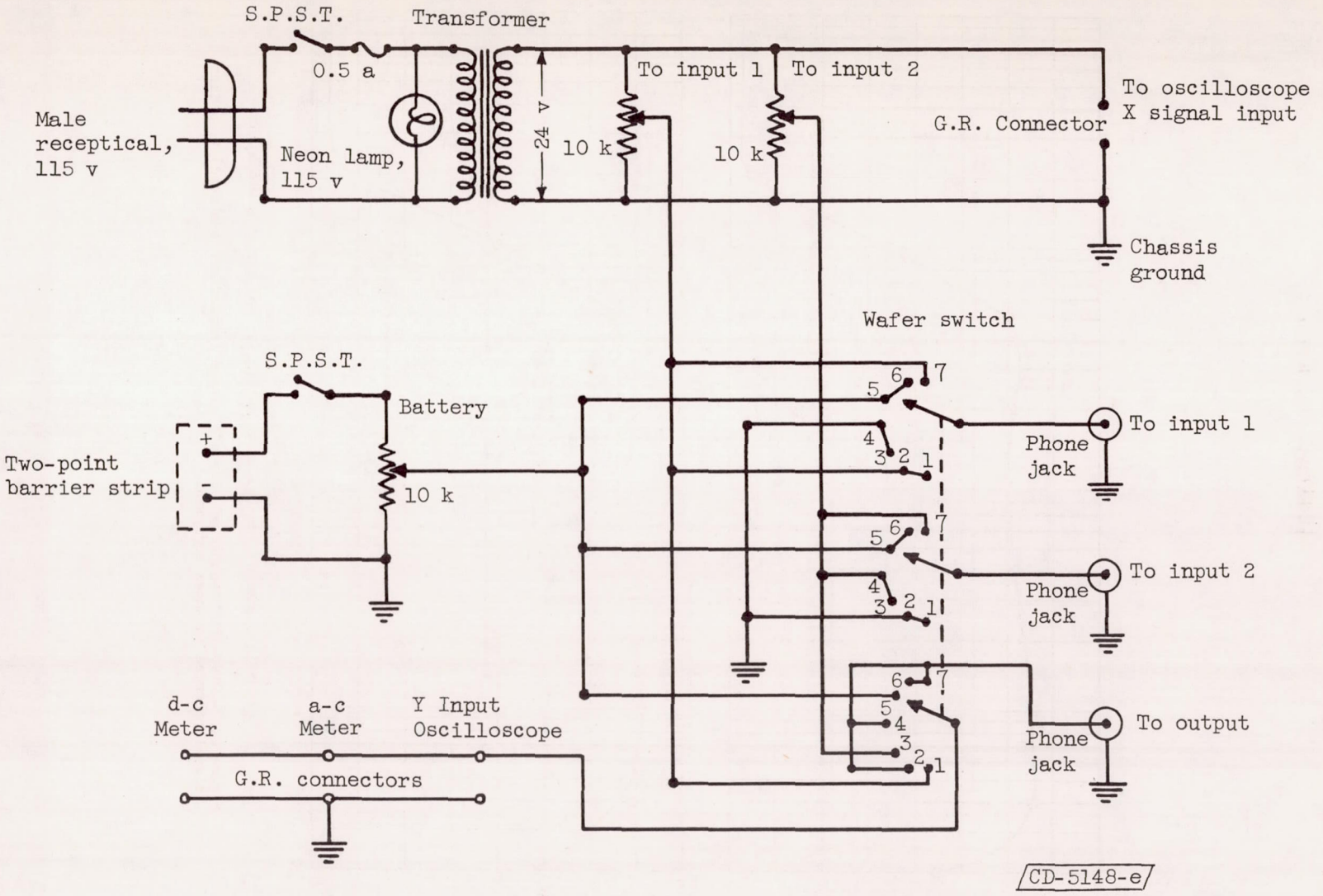

Figure 25. - Calibration circuit for Philbrick multiplier.

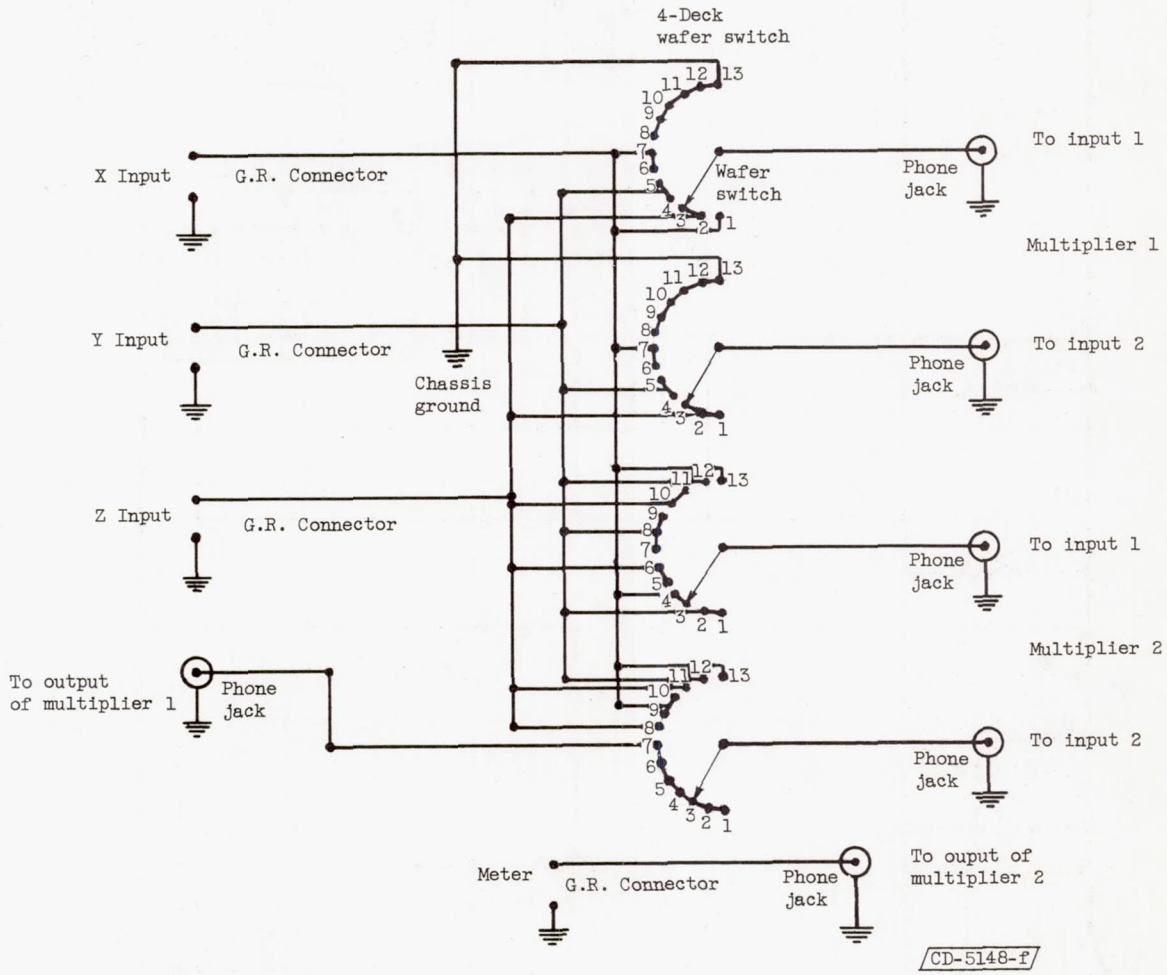

Figure 26. - Switching circuit for Philbrick multiplier for triple correlation.

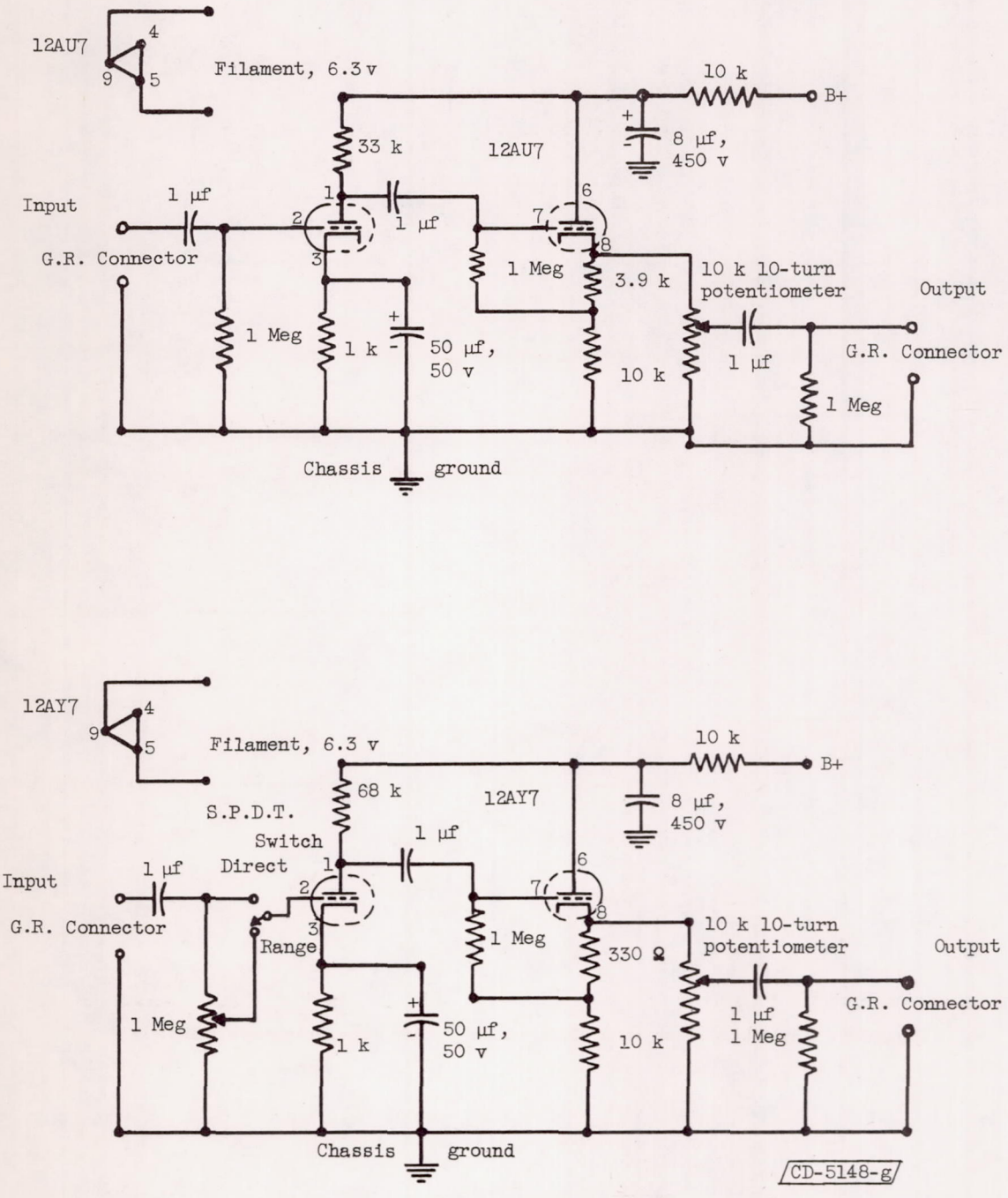

Figure 27. - Preamplifier circuits.